

Dual Quaternion SE(3) Synchronization with Recovery Guarantees

Jianing Zhao^{†1}, Linglingzhi Zhu^{†*2}, and Anthony Man-Cho So¹

¹Department of Systems Engineering and Engineering Management, The Chinese University of Hong Kong

²H. Milton Stewart School of Industrial and Systems Engineering, Georgia Institute of Technology

February 3, 2026

Abstract

Synchronization over the special Euclidean group $SE(3)$ aims to recover absolute poses from noisy pairwise relative transformations and is a core primitive in robotics and 3D vision. Standard approaches often require multi-step heuristic procedures to recover valid poses, which are difficult to analyze and typically lack theoretical guarantees. This paper adopts a dual quaternion representation and formulates $SE(3)$ synchronization directly over the unit dual quaternion. A two-stage algorithm is developed: A spectral initializer computed via the power method on a Hermitian dual quaternion measurement matrix, followed by a dual quaternion generalized power method (DQGPM) that enforces feasibility through per-iteration projection. The estimation error bounds are established for spectral estimators, and DQGPM is shown to admit a finite-iteration error bound and achieves linear error contraction up to an explicit noise-dependent threshold. Experiments on synthetic benchmarks and real-world multi-scan point-set registration demonstrate that the proposed pipeline improves both accuracy and efficiency over representative matrix-based methods.

1 Introduction

Global coordinate alignment, the task of unifying a network of local reference frames into a single and consistent global coordinate system, lies at the heart of 3D spatial perception. Whether reconstructing a trajectory in robotics or merging partial 3D scans in computer vision, the fundamental challenge is to recover the absolute poses (rotations and translations) of a set of nodes given only noisy measurements of their relative transformations. Mathematically formalized as synchronization over the special Euclidean group $SE(3)$, this problem serves as the foundation for diverse applications, including simultaneous localization and mapping (SLAM) (Liu et al., 2012; Rosen et al., 2019; Fan and Murphey, 2022), multiple point-set registration (Fusiello et al., 2002; Sharp et al., 2004; Arrigoni et al., 2016a), and structure from motion (SfM) (Govindu, 2004; Martinec and Pajdla, 2007). A prime example is multiple point-set registration, where the objective is to align a collection of 3D scans into a unified coordinate system. While early point-based approaches (Benjema and Schmitt, 1998; Zhou et al., 2016; Han et al., 2019) attempted to optimize point-to-point correspondences directly, they often suffer from prohibitive computational costs and susceptibility to local minima when initializations are poor. Consequently, modern pipelines favor frame-space methods (Chaudhury et al., 2015; Arrigoni et al., 2016a). These approaches decouple the problem into two steps: first, estimating pairwise relative transformations (e.g., via Iterative Closest Point (Besl and McKay, 1992)); second, globally synchronizing these noisy measurements to recover absolute poses. This abstraction effectively casts the registration task as an $SE(3)$ synchronization problem (Jiang et al., 2013; Özyesil and Singer, 2015).

*Corresponding author: llzzhu@gatech.edu

[†]Equal contribution.

Table 1: Rounding and Eigenspace–Synchronization Gap Across Groups

Group	Rounding / Projection	Eigenspace–Sync Gap
SO(2)	$z_i \leftarrow z_i / z_i $	$\text{Iso}(E)^* \cong \text{SO}(2) \Rightarrow \text{No gap}$
SO(d)	$\mathbf{G}_i \leftarrow \mathbf{U}_i \text{diag}(1, \dots, 1, \det(\mathbf{U}_i \mathbf{V}_i^\top)) \mathbf{V}_i^\top$	$\text{Iso}(E) \cong \text{O}(d) \Rightarrow \text{Moderate gap}$
SE(3)	Multi-step heuristic	$\text{Iso}(E)$ compact vs. non-compact $\text{SE}(3) \Rightarrow \text{Large mismatch}$

^{*} For the dominant eigenspace E , $\text{Iso}(E)$ denotes the group of linear isometries.

Consequently, the core task reduces to recovering the rigid motions (rotations and translations) that best satisfy a network of noisy relative constraints. Standard approaches typically represent $\text{SE}(3)$ elements using matrix embeddings:

$$\begin{pmatrix} \mathbf{R} & \mathbf{t} \\ \mathbf{0}^\top & 1 \end{pmatrix} \in \mathbb{R}^{4 \times 4},$$

where $\mathbf{R} \in \text{SO}(3)$ and $\mathbf{t} \in \mathbb{R}^3$. To address the non-convexity of the rank and orthogonality constraints, spectral relaxation (Arie-Nachimson et al., 2012; Arrigoni et al., 2016b) and semidefinite relaxation (SDR) (Liu et al., 2012; Chaudhury et al., 2015; Rosen et al., 2019) are widely employed. Additionally, Lie-algebraic averaging techniques (Govindu, 2004) and Riemannian optimization methods (Tron and Daniilidis, 2014) have also been applied to recover rigid motions.

However, matrix-based representations suffer from a fundamental limitation on the representation gap. Ideally, a group representation should align the isometry group of the nonzero eigenspace with the intrinsic global gauge symmetry of the synchronization problem. This alignment is essentially perfect for $\text{SO}(2)$ under the unit complex representation: the eigenspace isometry matches $\text{SO}(2)$, making rounding a trivial normalization. For $\text{SO}(d)$, the eigenspace isometry expands to $\text{O}(d)$, introducing only a mild gap (a reflection ambiguity) that is rigorously resolved via SVD projection. In contrast, as summarized in Table 1, the conventional 4×4 matrix representation of $\text{SE}(3)$ breaks this favorable correspondence. While the relaxed eigenspace possesses a compact orthogonal geometry, $\text{SE}(3) = \text{SO}(3) \ltimes \mathbb{R}^3$ is inherently non-compact. Consequently, the relaxed solution often lies far from the manifold, creating a large eigenspace-sync gap. Rounding is no longer a benign projection that merely corrects noise; instead, it must artificially enforce a group structure absent from the eigenspace geometry. This necessitates complex, multi-step heuristic procedures that are often unstable (Arrigoni et al., 2016b; Rosen et al., 2019). Although alternative representations exist, such as axis-angle pairs (Thunberg et al., 2014; Jin et al., 2020), augmented unit quaternions (Grisetti et al., 2010; Chen et al., 2024), and dual quaternions (Cheng et al., 2016; Srivatsan et al., 2016; Hadi et al., 2024) exist, they typically lack a unified algebraic framework that is both compact and amenable to rigorous optimization guarantees.

In this paper, we adopt the dual quaternion representation of $\text{SE}(3)$. Practically, this choice leads to a simpler and more stable rounding/projection step. Conceptually, it aligns the spectral ambiguity more closely with the intrinsic gauge symmetry of $\text{SE}(3)$, thereby mitigating the eigenspace–synchronization mismatch induced by matrix embeddings. Specifically, we represent each pose by a unit dual quaternion and work over the constraint set $\text{UDQ} := \{x \in \mathbb{DH} : |x| = 1\}$. Given noisy relative measurements, we estimate the unknown poses $\hat{\mathbf{x}} = (\hat{x}_1, \dots, \hat{x}_n) \in \text{UDQ}^n$ by solving the least-squares problem

$$\arg \min_{x \in \text{UDQ}^n} \sum_{1 \leq i < j \leq n} |C_{ij} - x_i x_j^*|^2, \quad (1.1)$$

where \mathbb{DH} denotes the algebra of dual quaternions and $(\cdot)^*$ is the conjugate transpose, which coincides

with the group inverse on UDQ . The measurement matrix $C \in \mathbb{DH}^{n \times n}$ is Hermitian with entries

$$C_{ij} = \hat{x}_i \hat{x}_j^* + \Delta_{ij}, \quad 1 \leq i < j \leq n, \quad (1.2)$$

and $\Delta \in \mathbb{DH}^{n \times n}$ collects the Hermitian observation noise.

To efficiently tackle the nonconvex optimization problem (1.1), we build on the generalized power method (GPM) and develop a two-stage framework that combines a provably accurate spectral initializer with an iterative refinement scheme that preserves feasibility at every step. Variants of this spectral initializer with an iterative refinement strategy have proved effective for phase, orthogonal, and rotation group synchronization problems (Boumal, 2016; Ling, 2022; Liu et al., 2023; Zhu et al., 2023). However, establishing rigorous guarantees in the dual quaternion setting is substantially more challenging. First, dual quaternions form a ring with zero divisors rather than a field, so division is not generally well defined. Second, as the natural modulus on dual quaternions is merely a dual-number valued seminorm, a bounded modulus does not imply bounded components. This allows translations to grow arbitrarily large despite a finite modulus, thereby posing challenges for stability and convergence analysis. Third, identifying a dominant eigenpair typically invokes the lexicographic order on dual numbers, whereas estimation and convergence are naturally quantified in Euclidean metrics. By addressing these theoretical hurdles, we provide the first recovery guarantees for synchronization over the dual quaternion. Our main contributions are as follows:

- SE(3) synchronization is formulated as a least-squares problem over unit dual quaternions UDQ^n with a Hermitian dual quaternion measurement matrix. We formalize a normalization/projection map onto UDQ , establish its stability (a Lipschitz-type bound), and provide a closed-form componentwise projection onto UDQ^n . These results transform the rounding step, often a heuristic in matrix-based methods, into a well-posed and quantitatively controllable operation that underpins our recovery analysis.
- The spectral initialization scheme is developed by computing the dominant eigenvector of a Hermitian dual quaternion measurement matrix via the power method, and then applying an elementwise projection to enforce feasibility in UDQ^n . In contrast to heuristic initializations, we establish nonasymptotic estimation error guarantees for both the raw (generally infeasible) spectral estimator and its projected, feasible counterpart (Proposition 2.4 and Theorem 2.8). These bounds ensure that the initializer lies within a controlled neighborhood of the ground truth under operator norm noise, placing it inside the basin of attraction needed for subsequent GPM refinement and thereby reducing the risk of convergence to undesirable local minima.
- We propose a dual quaternion generalized power method (DQGPM) to refine the spectral initializer while strictly enforcing the unit dual quaternion constraints. Specifically, DQGPM applies an elementwise projection onto UDQ^n at every iteration, yielding a stop-anytime feasible iterate sequence. Under a mild noise regime and a sufficiently accurate initialization, we prove that the estimation error contracts at a linear rate up to an explicit error floor (Theorem 3.2). To the best of our knowledge, this provides the first finite-iteration recovery guarantee for SE(3) synchronization, especially for the dual quaternion formulation.

We evaluate our framework on both synthetic datasets and real-world multiple point-set registration tasks. Our results demonstrate that the proposed method significantly outperforms matrix-based approaches, including spectral relaxation and semidefinite relaxation, achieving higher recovery accuracy with greater computational efficiency.

1.1 Notation

Throughout the paper, the sets of dual numbers, quaternions, and dual quaternions are denoted by \mathbb{D} , \mathbb{H} , and \mathbb{DH} , respectively. For a dual number $a = a_{st} + a_{\mathcal{I}}\epsilon$ with $a_{st} \neq 0$, its inverse is $a^{-1} = a_{st}^{-1}(1 - a_{\mathcal{I}}a_{st}^{-1}\epsilon)$.

The operator $(\cdot)^*$ denotes the (dual) quaternion conjugate when applied to a scalar element, and the conjugate transpose when applied to a vector or matrix. The scalar part of a quaternion q is denoted by $\text{sc}(q) = \frac{1}{2}(q + q^*)$. For two n -dimensional (dual) quaternion vectors $\mathbf{x} = (x_1, \dots, x_n)$ and $\mathbf{y} = (y_1, \dots, y_n)$, their inner product is defined as $\mathbf{x}^* \mathbf{y} = \sum_{i=1}^n x_i^* y_i$. The Frobenius norm of a (dual) quaternion matrix is denoted by $\|\cdot\|_F$, which reduces to the 2-norm $\|\cdot\|_2$ for a (dual) quaternion vector. The operator norm of a (dual) quaternion matrix is denoted by $\|\cdot\|_{\text{op}}$. The set of unit dual quaternions is denoted by $\text{UDQ} := \{q \in \mathbb{DH} : qq^* = 1\}$. We write $\text{UDQ}^n := \{\mathbf{x} = (x_1, \dots, x_n) : x_i \in \text{UDQ}\}$, that is, the set of n -dimensional vectors whose entries are unit dual quaternions. For $\mathbf{x} \in \mathbb{DH}^n$, the element-wise projection onto UDQ^n is defined by $\Pi(\mathbf{x}) = \operatorname{argmin}_{\mathbf{u} \in \text{UDQ}^n} \|\mathbf{u} - \mathbf{x}\|_2^2$. For any $\mathbf{x}, \mathbf{y} \in \mathbb{DH}^n$, the distance between them, defined up to a global unit dual quaternion alignment, is given by $d(\mathbf{x}, \mathbf{y}) = \min_{z \in \text{UDQ}} \|\mathbf{x} - \mathbf{y}z\|_2$. We denote by $d_{st}(\mathbf{x}, \mathbf{y})$ and $d_{\mathcal{I}}(\mathbf{x}, \mathbf{y})$ the standard part and the imaginary part of $d(\mathbf{x}, \mathbf{y})$, respectively. For $z \in \mathbb{DH}$, we denote the normalization of z onto UDQ as $\mathcal{N}(z)$. Given $\{a_k\} \subset \mathbb{D}$ and $\{c_k\} \subset \mathbb{R}$, we define $a_k = O_{\mathbb{D}}(c_k)$ iff $(a_k)_{st} = O(c_k)$ and $(a_k)_{\mathcal{I}} = O(c_k)$.

2 Spectral Estimator

The least-squares Problem (1.1) can be reformulated as an equivalent quadratic program with quadratic constraints (QPQC) over unit dual quaternions:

$$\min_{\mathbf{x} \in \text{UDQ}^n} \|\mathbf{C} - \mathbf{x}\mathbf{x}^*\|_F^2. \quad (2.1)$$

This reformulation naturally leads to a spectral related problem based on the dominant eigenvectors of the dual quaternion Hermitian matrix \mathbf{C} .

Proposition 2.1 (Equivalent QPQC Formulation). *For a Hermitian dual quaternion matrix $\mathbf{C} \in \mathbb{DH}^{n \times n}$, Problem (2.1) is equivalent to*

$$\arg \max_{\mathbf{x} \in \text{UDQ}^n} \mathbf{x}^* \mathbf{C} \mathbf{x}, \quad (\text{P})$$

and their optimal objective values differ only by a multiplicative factor of 2.

The maximization problem (P) is nonconvex and can be challenging to solve directly. Nevertheless, by slightly relaxing the constraints, we obtain the following natural spectral relaxation, which reduces the computation to a leading-eigenvectors problem:

$$\arg \max_{\mathbf{x} \in \mathbb{DH}^n, \|\mathbf{x}\|_2^2=n} \mathbf{x}^* \mathbf{C} \mathbf{x} \quad (2.2)$$

Fact 2.2 (Ling et al. (2022, Lemma 4.2)). Let $\mathbf{C} \in \mathbb{DH}^{n \times n}$ be a Hermitian matrix and λ_1 be the largest right eigenvalue of \mathbf{C} with associated right eigenvector $\mathbf{u}_1 \in \mathbb{DH}^n$. Then

$$\lambda_1 = \max \{ \|\mathbf{x}\|^{-2} (\mathbf{x}^* \mathbf{C} \mathbf{x}) \mid \mathbf{x} \in \mathbb{DH}^n \setminus \{\mathbf{0}\} \},$$

and the maximum is attained at $\mathbf{x} = \mathbf{u}_1$.

By Fact 2.2, the optimum of (2.2) is attained at the dominant right eigenvector \mathbf{u}_1 of \mathbf{C} , normalized so that $\|\mathbf{u}_1\|_2^2 = n$. Recently, Cui and Qi (2024) proposed a power iteration method for computing the dominant eigenvalue and a corresponding eigenvector of a dual quaternion Hermitian matrix, and established linear convergence of the resulting iterates to the dominant eigenpair. The procedure is summarized in Algorithm 1.

Remark 2.3 (Well-definedness of the Inverse). The mild assumption $\lambda_{1,st} \neq 0$ and $(\mathbf{w}_{st}^0)^* \mathbf{u}_{1,st} \neq 0$ ensures that dominant eigenspace exists and the initialization has a nonzero standard part projection onto the dominant eigenspace. If $(\mathbf{w}_{st}^0)^* \mathbf{u}_{1,st} = 0$, then the power iteration cannot amplify (and hence cannot converge to) the dominant eigenspace. Under these assumptions, the standard part iterate remains nonzero, i.e., $\mathbf{y}_{st}^k \neq \mathbf{0}$, making the inverse well-defined.

Algorithm 1 Power Iteration for Eigenvector Estimator

- 1: **Input:** Hermitian matrix $\mathbf{C} \in \mathbb{DH}^{n \times n}$ with dominant right eigenvalue λ_1 satisfying $\lambda_{1,st} \neq 0$, random initial point $\mathbf{w}^0 \in \mathbb{DH}^n$ such that $(\mathbf{w}_{st}^0)^* \mathbf{u}_{1,st} \neq 0$.
 - 2: **for** $k = 1, 2, \dots$ **do**
 - 3: $\mathbf{y}^k = \mathbf{C}\mathbf{w}^{k-1}$.
 - 4: $\mathbf{w}^k = \mathbf{y}^k \cdot (\|\mathbf{y}^k\|_2)^{-1}$.
 - 5: **end for**
 - 6: **Output:** $\sqrt{n} \mathbf{w}^{k-1}$.
-

We next characterize the estimation error of this spectral estimator to the ground truth $\hat{\mathbf{x}}$.

Proposition 2.4 (Eigenvector Estimation Error). *Let $\mathbf{x} \in \mathbb{DH}^n$ satisfy $\|\mathbf{x}\|_2^2 = n$ and $\mathbf{x}^* \mathbf{C} \mathbf{x} \geq \hat{\mathbf{x}}^* \mathbf{C} \hat{\mathbf{x}}$. Then*

$$d(\mathbf{x}, \hat{\mathbf{x}}) \leq \frac{4\|\Delta\|_{\text{op}}}{\sqrt{n}}.$$

Proposition 2.4 shows that the dominant eigenvector \mathbf{u}_1 of \mathbf{C} , normalized to satisfy $\|\mathbf{u}_1\|_2^2 = n$, is close to the ground truth $\hat{\mathbf{x}}$. However, \mathbf{u}_1 does not necessarily lie in UDQ^n . To obtain a feasible initializer, we therefore apply an element-wise projection of \mathbf{u}_1 onto UDQ^n .

We first define the normalization operator $\mathcal{N}(\cdot)$, which maps a dual quaternion $x \in \mathbb{DH}$ to a unit dual quaternion $\mathcal{N}(x) \in \text{UDQ}$. Let $u := \mathcal{N}(x)$. If $x_{st} \neq 0$, then

$$u_{st} = \frac{x_{st}}{|x_{st}|}, \quad u_{\mathcal{I}} = \frac{x_{\mathcal{I}}}{|x_{st}|} - \frac{x_{st}}{|x_{st}|} \text{sc} \left(\frac{x_{st}^*}{|x_{st}|} \frac{x_{\mathcal{I}}}{|x_{st}|} \right).$$

If $x_{st} = 0$ and $x_{\mathcal{I}} \neq 0$, then

$$u_{st} = \frac{x_{\mathcal{I}}}{|x_{\mathcal{I}}|}, \quad u_{\mathcal{I}} \text{ is any quaternion satisfying } \text{sc}(x_{\mathcal{I}}^* u_{\mathcal{I}}) = 0.$$

Next, we record a stability property of the normalization map $\mathcal{N}(\cdot)$. It shows that normalizing a dual quaternion cannot increase its distance to any unit dual quaternion by more than a constant factor. This bound will be used repeatedly to transfer error bounds from the (possibly infeasible) eigenvector \mathbf{u}_1 to its element-wise projection onto UDQ^n .

Lemma 2.5 (Lipschitz Property of \mathcal{N}). *For any $y \in \mathbb{DH}$ and any $z \in \text{UDQ}$, we have*

$$|\mathcal{N}(y) - z| \leq 2|y - z|.$$

Remark 2.6. Related results were established in [Liu et al. \(2017\)](#) for the special case of $\text{SO}(2)$, where the proof exploits algebraic properties of complex numbers. A more general treatment for the $\text{O}(d)$ group was given in [Liu et al. \(2023\)](#), with arguments based on the definition of projection rather than an explicit normalization map. In contrast, our proof relies only on the algebraic properties of dual quaternions. Nevertheless, normalization and projection coincide in an important sense. In particular, [Cui and Qi \(2024, Theorem 3.1\)](#) shows that for any $x \in \mathbb{DH}$, the normalized dual quaternion $u = \mathcal{N}(x)$ is the metric projection of x onto UDQ , namely

$$\mathcal{N}(x) \in \arg \min_{u \in \text{UDQ}} |u - x|^2.$$

Consequently, Lemma 2.5 can also be proved using standard properties of metric projections.

The following result shows that the projection of a dual quaternion vector \mathbf{y} onto UDQ^n , denoted by $\Pi(\mathbf{y})$, admits a closed-form expression.

Proposition 2.7 (Projection onto UDQ^n). *For any $\mathbf{y} \in \mathbb{DH}^n$, define*

$$\tilde{\mathbf{y}} = \begin{cases} \mathcal{N}(y_i) & \text{if } y_i \neq 0, \\ \mathcal{N}(\mathbf{e}^* \mathbf{y}) & \text{otherwise,} \end{cases}$$

where $\mathbf{e} \in \mathbb{DH}^n$ is any vector satisfying $\mathbf{e}^* \mathbf{y} \neq 0$. If $\mathbf{y} = \mathbf{0}$, we set $\tilde{\mathbf{y}} = \mathbf{1}^n$. Then $\tilde{\mathbf{y}}$ is the projection of \mathbf{y} onto UDQ^n , i.e., $\tilde{\mathbf{y}} = \Pi(\mathbf{y})$.

With the component-wise projection in Proposition 2.7, we can define an alternative feasible estimator

$$\tilde{\mathbf{x}} := \Pi(\mathbf{u}_1), \quad (2.3)$$

which lies in UDQ^n by construction. We next show that $\tilde{\mathbf{x}}$ remains close to the ground-truth signal $\hat{\mathbf{x}}$.

Theorem 2.8 (Rounded Spectral Estimation Error). *For $\tilde{\mathbf{x}}$ given by (2.3), we have*

$$d(\tilde{\mathbf{x}}, \hat{\mathbf{x}}) \leq \frac{8\|\Delta\|_{\text{op}}}{\sqrt{n}}.$$

Theorem 2.8 follows from the Lipschitz property of the normalization/projection map in Lemma 2.5. In particular, it implies that $\tilde{\mathbf{x}}$ achieves the same order of accuracy as the (generally infeasible) spectral solution \mathbf{u}_1 to (2.2), while ensuring feasibility in UDQ^n .

3 Iterative Estimation Performance

Although Proposition 2.4 and Theorem 2.8 show that both the (infeasible) spectral solution of (2.2) and its rounded version yield accurate estimates close to the ground-truth signal, these estimators alone do not directly solve (2.1) beyond serving as a starting point. To obtain a fully iterative refinement procedure whose iterates remain feasible, we develop a *dual quaternion generalized power method* (DQGPM) as the second-stage algorithm.

The GPM was originally proposed by Journée et al. (2010) for maximizing a convex function over a compact set via a power-type iteration combined with a projection step. Specializing this idea to the synchronization problem (P), our method applies an element-wise projection onto UDQ^n at every iteration, thereby ensuring feasibility throughout the run. In contrast to eigenvector-based estimators (which only become feasible after a final rounding step), DQGPM can be stopped at any iterate, and the intermediate estimate is always feasible for (P).

Algorithm 2 Dual Quaternion Generalized Power Method

```

1: Input: Hermitian matrix  $\mathbf{C} \in \mathbb{DH}^{n \times n}$ , initializer  $\mathbf{x}^0 = \mathbf{u}_1 \in \mathbb{DH}^n$ .
2: for  $k = 1, 2, \dots$  do
3:    $\mathbf{y}^k = \mathbf{C} \mathbf{x}^{k-1}$ 
4:    $\mathbf{x}^k = \Pi(\mathbf{y}^k)$ 
5: end for
6: Output:  $\mathbf{x}^k$ .

```

The following Theorem 3.2 shows that, under mild noise conditions and a sufficiently accurate initializer, the DQGPM iterates contract toward the ground truth at a linear rate up to an $O(\|\Delta \hat{\mathbf{x}}\|_2/n)$ error floor.

Remark 3.1 (Algebraic Order vs. Estimation Metric). We need to distinguish the algebraic order used in Section 2 from the error metric used in our convergence analysis. While the spectral estimator relies on the lexicographical order of dual numbers to define the dominant eigenpair (strictly prioritizing the standard

part), $\text{SE}(3)$ synchronization requires bounded errors in both rotation and translation. Therefore, in this section, we analyze the estimation error by controlling the real-valued magnitudes of the standard component d_{st} and the dual component $d_{\mathcal{I}}$ individually. This component-wise analysis is consistent with the algebraic structure of dual numbers, where the convergence of the dual part ($d_{\mathcal{I}}$) typically depends on the accuracy of the standard part (d_{st}).

Theorem 3.2 (Estimation Error of DQGPM). *Suppose that the measurement noise satisfies $\|\Delta\|_{\text{op},st} \leq n/350$, $\|\Delta\|_{\text{op},\mathcal{I}} \leq n/300$, and the initialization is given by $\mathbf{x}^0 = \mathbf{u}_1$. Then the sequence generated by Algorithm 2 satisfies*

$$d_{st}(\mathbf{x}^k, \hat{\mathbf{x}}) \leq \left(\frac{1}{10}\right)^k d_{st}(\mathbf{x}^0, \hat{\mathbf{x}}) + \frac{700}{53n} \|\Delta \hat{\mathbf{x}}\|_{2,st}, \quad (3.1)$$

and

$$d_{\mathcal{I}}(\mathbf{x}^k, \hat{\mathbf{x}}) \leq \left(\frac{1}{10}\right)^k d_{\mathcal{I}}(\mathbf{x}^0, \hat{\mathbf{x}}) + k \left(\frac{1}{10}\right)^{k-1} \frac{1}{8} d_{st}(\mathbf{x}^0, \hat{\mathbf{x}}) + \frac{700}{53n} \|\Delta \hat{\mathbf{x}}\|_{2,\mathcal{I}} + \frac{875}{477n} \|\Delta \hat{\mathbf{x}}\|_{2,st}. \quad (3.2)$$

Remark 3.3. It is worth noting the improvement in estimation accuracy provided by DQGPM over the rounded spectral estimator. Theorem 3.2 establishes that, asymptotically as $k \rightarrow \infty$ (assuming a small noise constant regime where $\|\Delta\|_{\text{op},st}, \|\Delta\|_{\text{op},\mathcal{I}} \leq an$ for sufficiently small $a > 0$), the DQGPM estimation error satisfies:

$$d_{st}(\mathbf{x}^{\infty}, \hat{\mathbf{x}}) \lesssim \frac{12}{n} \|\Delta \hat{\mathbf{x}}\|_{2,st}, \quad d_{\mathcal{I}}(\mathbf{x}^{\infty}, \hat{\mathbf{x}}) \lesssim \frac{12}{n} \|\Delta \hat{\mathbf{x}}\|_{2,\mathcal{I}}.$$

In contrast, Theorem 2.8 guarantees an error bound for the rounded spectral estimator of order $8\|\Delta\|_{\text{op}}/\sqrt{n}$. Comparing these rates, DQGPM yields a tighter bound provided that $\|\Delta \hat{\mathbf{x}}\|_{2,st} \leq c\sqrt{n}\|\Delta\|_{\text{op},st}$ and $\|\Delta \hat{\mathbf{x}}\|_{2,\mathcal{I}} \leq c\sqrt{n}\|\Delta\|_{\text{op},\mathcal{I}}$ for a constant $c < 2/3$. Note that the trivial bound $c = 1$ holds automatically by definition. In many stochastic noise models, however, $\hat{\mathbf{x}}$ is not aligned with the top singular directions of Δ , so $\|\Delta \hat{\mathbf{x}}\|_2$ is typically much smaller than the worst-case bound (e.g., $c \approx 1/2$ for standard i.i.d. Gaussian noise), which highlights the advantage of the DQGPM refinement.

Finally, since the dominant eigenvector \mathbf{u}_1 cannot be computed exactly in practice, we quantify the following finite-iteration estimation error of the two-stage procedure power iteration for initialization followed by DQGPM refinement.

Corollary 3.4 (Finite-Iteration Estimation Error). *Suppose the noise assumptions in Theorem 3.2 hold. Let $\mathbf{C} \in \mathbb{DH}^{n \times n}$ be Hermitian and admits a unique dominant eigenvalue with multiplicity one. Denote its right eigenvalues by $\lambda_1 > \lambda_2 \geq \dots \geq \lambda_n$, where each $\lambda_i = \lambda_{i,st} + \lambda_{i,\mathcal{I}}\epsilon$ is a dual number. If we run Algorithm 1 for K_{init} iterations satisfying*

$$K_{\text{init}} \geq \max \left\{ \log_r \left(\frac{35|\alpha_{2,st}| + 34M_{st}}{|\alpha_{1,st}|} \right), \log_r \left(\frac{25N_2 + 24M_{\mathcal{I}}}{N_1} \right) \right\},$$

then, initializing Algorithm 2 with $\mathbf{x}^0 := \sqrt{n} \mathbf{w}^{K_{\text{init}}}$, the resulting sequence $\{\mathbf{x}^k\}_{k \geq 0}$ satisfies:

$$d_{st}(\mathbf{x}^k, \hat{\mathbf{x}}) \leq \left(\frac{1}{10}\right)^k \frac{\sqrt{n}}{25} + \frac{700}{53n} \|\Delta \hat{\mathbf{x}}\|_{2,st},$$

and

$$d_{\mathcal{I}}(\mathbf{x}^k, \hat{\mathbf{x}}) \leq \left(\frac{1}{10}\right)^k \frac{\sqrt{n}}{18} + k \left(\frac{1}{10}\right)^{k-1} \frac{\sqrt{n}}{200} + \frac{700}{53n} \|\Delta \hat{\mathbf{x}}\|_{2,\mathcal{I}} + \frac{875}{477n} \|\Delta \hat{\mathbf{x}}\|_{2,st}.$$

Here $r := |\lambda_{1,st}/\lambda_{2,st}| > 1$, $M_{st}, M_{\mathcal{I}}, N_1, N_2$ are some real constants depending on $\alpha_1, \lambda_1, \lambda_2$, and α_1 is the projection of initializer \mathbf{w}^0 onto normalized dominant eigenvector.

Table 2: Rotation and translation errors of DQGPM and EIG across noise levels and observation rates.

NOISE LEVEL		(0.05, 5°)	(0.10, 10°)	(0.15, 15°)	(0.20, 20°)
$p = 0.05$	ERROR_R	DQGPM	0.034 ± 0.051	0.035 ± 0.051	0.036 ± 0.050
		EIG	0.056 ± 0.632	0.050 ± 0.183	0.052 ± 0.130
	ERROR_T	DQGPM	0.069 ± 0.043	0.132 ± 0.064	0.196 ± 0.088
		EIG	0.580 ± 1.924	0.662 ± 1.982	0.739 ± 5.556
$p = 0.08$	ERROR_R	DQGPM	0.001 ± 0.008	0.002 ± 0.008	0.003 ± 0.008
		EIG	0.001 ± 0.625	0.003 ± 0.013	0.004 ± 0.006
	ERROR_T	DQGPM	0.032 ± 0.007	0.064 ± 0.009	0.095 ± 0.012
		EIG	0.042 ± 0.676	0.085 ± 0.814	0.128 ± 0.922
$p = 0.30$	ERROR_R	DQGPM	0.0005 ± 0.000	0.001 ± 0.000	0.001 ± 0.000
		EIG	0.001 ± 0.000	0.001 ± 0.000	0.002 ± 0.625
	ERROR_T	DQGPM	0.013 ± 0.001	0.027 ± 0.001	0.040 ± 0.002
		EIG	0.015 ± 0.033	0.031 ± 0.130	0.047 ± 0.113

* 15% trimmed means reported (due to EIG instability);
SDR excluded due to limited scalability under uniform edge dropout.

4 Numerical Experiments

In this section, we report the recovery performance and numerical efficiency of our propose DQGPM for SE(3) synchronization tasks on both synthetic and real data, where the real data experiments are implemented on multiple point-set registration problem. We also compare our method with two existing matrix-based methods, which are the spectral decomposition (EIG) described in [Arrigoni et al. \(2016b\)](#), and the semidefinite relaxation (SDR) approach introduced in [Rosen et al. \(2019\)](#). All experiments were performed in Python 3.9 on a computer running Windows 11, equipped with an AMD Ryzen 7 6800HS Creator Edition (3.20 GHz) processor and 16 GB of RAM. Experimental results on synthetic data with additive noise are presented in Section 4.2, while Section 4.3 reports results obtained from real data in the multiple point-set registration experiment.

4.1 Data Generation and Evaluation Metrics

Data Generation We construct synthetic experiments by simulating a noisy measurement matrix \mathbf{C} under the additive model

$$\mathbf{C} = \hat{\mathbf{x}}\hat{\mathbf{x}}^* + \Xi - \mathbf{1}_{n \times n}.$$

Here, $\hat{\mathbf{x}} = (\hat{x}_1, \dots, \hat{x}_n) \in \text{UDQ}^n$ is the ground-truth pose vector, and term $\Xi = (\xi_{ij}) \in \text{UDQ}^{n \times n}$ is a Hermitian dual quaternion noise matrix, all their entries are sampled i.i.d. as unit dual quaternions. The matrix $\mathbf{1}_{n \times n}$ denotes the all-one dual quaternion matrix. The term $\Xi - \mathbf{1}_{n \times n}$ corresponds to the additive noise Δ in the model (1.2).

To evaluate robustness under partial observation, we sparsify the measurements using an Erdős–Rényi (ER) graph $\mathbf{E} = (e_{ij})$, where $e_{ij} \sim \text{Bernoulli}(p)$ and p controls the observation rate. The resulting simulated measurement matrix \mathbf{C} is defined entrywise as

$$C_{ij} = \begin{cases} e_{ij}(\hat{x}_i\hat{x}_j^* + \xi_{ij} - 1), & 1 \leq i < j \leq n, \\ 1, & i = j, \\ C_{ji}^*, & 1 \leq j < i \leq n. \end{cases}$$

We subtract $\mathbf{1}_{n \times n}$ for two reasons. First, since ξ_{ij} is a unit dual quaternion, adding it directly to $\hat{x}_i \hat{x}_j^*$ can inflate the entry magnitude and distort the signal. Second, in dual quaternions the motion-free baseline is the identity element (an all-ones matrix), not zero. Therefore, we use the shifted model and subtract $\mathbf{1}_{n \times n}$.

To represent elements in $\text{SE}(3)$ for both the ground-truth poses and the noise terms, we sample $(\mathbf{u}, \theta, \mathbf{t})$ to generate an unit dual quaternion x . Each sampled dual quaternion x is constructed from a random rotation represented by $q \in \mathbb{H}$ and translation $\mathbf{t} \in \mathbb{R}^3$: we first form the unit quaternion q from a randomly sampled axis $\mathbf{u} \in \mathbb{R}^3$ and angle $\theta \in [0, 2\pi)$ via (B.1), and generate a randomly sampled \mathbf{t} then convert (q, \mathbf{t}) to x using (B.2).

Evaluation Metrics We follow the evaluation and gauge-alignment procedure of [Hadi et al. \(2024\)](#). Define ground-truth poses as $\hat{\mathbf{x}} = \{(\hat{q}_i, \hat{t}_i)\}_{i=1}^n \in \text{SE}(3)^n$ and estimates as $\mathbf{x} = \{(q_i, t_i)\}_{i=1}^n \in \text{SE}(3)^n$, where $\hat{q}_i, q_i \in \mathbb{H}$ are unit quaternions and $\hat{t}_i, t_i \in \mathbb{R}^3$ are translations. We compute the estimation error as the distance between \mathbf{x} and the right-aligned ground-truth $\hat{\mathbf{x}}z$, where z is the optimal aligner that minimizes the distance between \mathbf{x} and $\hat{\mathbf{x}}z$. Specifically, we get the aligning $\text{SE}(3)$ element $z = (q, t)$ by

$$q = \frac{s}{\|s\|}, \quad t = \frac{1}{n} \sum_{j=1}^n \psi_{\hat{q}_j^*}(t_j - \hat{t}_j),$$

where $s = \sum_{j=1}^n \hat{q}_j^* q_j$, and $\psi : \mathbb{R}^3 \rightarrow \mathbb{R}^3$ denotes the action of the quaternion-induced rotation on vectors (see Proposition B.1 in the Appendix).

After alignment, we report rotation and translation errors for each estimated pose, following [Hadi et al. \(2024\)](#):

$$\begin{aligned} d_R(q_1, q_2) &= 2 \arccos(2 \langle q_1, q_2 \rangle^2 - 1), \\ d_T(t_1, t_2) &= \|t_1 - t_2\|_2, \end{aligned}$$

where $\langle \cdot, \cdot \rangle$ denotes the Euclidean inner product in \mathbb{R}^4 . We report `error_r` and `error_t` as the mean of d_R and d_T , respectively, over all n targets.

4.2 Recovery Performance and Computational Time

For each ground-truth pose \hat{x}_i , we sample the rotation axis \mathbf{u} uniformly from the unit sphere in \mathbb{R}^3 and the rotation angle independently and uniformly from $[0, 2\pi)$. The translation $\mathbf{t} = (t_1, t_2, t_3) \in \mathbb{R}^3$ has i.i.d. entries following $\mathcal{N}(0, 1)$. To generate the noise matrix, we again sample rotation axes uniformly from the unit sphere, while rotation angles (in degrees) are drawn i.i.d. from $\mathcal{N}(0, \sigma_r^2)$ with $\sigma_r \in \{5^\circ, 10^\circ, 15^\circ, 20^\circ\}$. The corresponding translation noise has i.i.d. entries drawn from $\mathcal{N}(0, \sigma_t^2)$ with $\sigma_t \in \{0.05, 0.10, 0.15, 0.2\}$, respectively.

We run synthetic experiments with problem size $n = 100$ under three observation rates

$$p \in \{0.05, 0.08, 0.3\},$$

corresponding to approximately 95%, 92%, and 70% missing pairs, respectively. For each setting, we execute Algorithm 1 until the residual drops below 10^{-5} , and then project the output elementwise onto UDQ^n . All results are averaged over 100 independent trials.

Table 2 reports the rotation and translation errors (`error_r`, `error_t`) of DQGPM and the baseline EIG across various noise levels and observation rates. The two metrics exhibit consistent trends, and DQGPM is uniformly more accurate and stable, with the largest gains in sparse graphs ($p = 0.05$). DQGPM maintains small errors across all noise levels, whereas EIG incurs larger errors with substantially higher variance. As the graph becomes denser ($p = 0.08$ and $p = 0.30$), both methods improve and the performance gap narrows; nonetheless, DQGPM continues to achieve lower errors and reduced variance, retaining a mild but consistent advantage in the dense regime. Besides, we record the total CPU time

Table 3: CPU time of DQGPM and EIG across noise levels and observation rates.

		(0.05, 5°)	(0.10, 10°)	(0.15, 15°)	(0.20, 20°)
$p = 0.05$	DQGPM	0.011	0.011	0.010	0.010
	EIG	0.014	0.014	0.015	0.014
$p = 0.08$	DQGPM	0.007	0.007	0.008	0.007
	EIG	0.014	0.011	0.013	0.011
$p = 0.30$	DQGPM	0.010	0.011	0.010	0.011
	EIG	0.017	0.017	0.017	0.019

consumed by each method in Table 3. It can be observed that DQGPM is consistently faster than EIG across all settings, and its runtime is insensitive to the noise level.

Figure 1 plots estimation error (`error_r` and `error_t`) versus iteration for different problem sizes n , indicating a linear error contraction of estimation error for GPM refinement stage. Within a small number of iterations, the decrease gradually saturates and the errors flatten at a nonzero plateau, which corresponds to the asymptotic noise floor as analyzed in Remark 3.3.

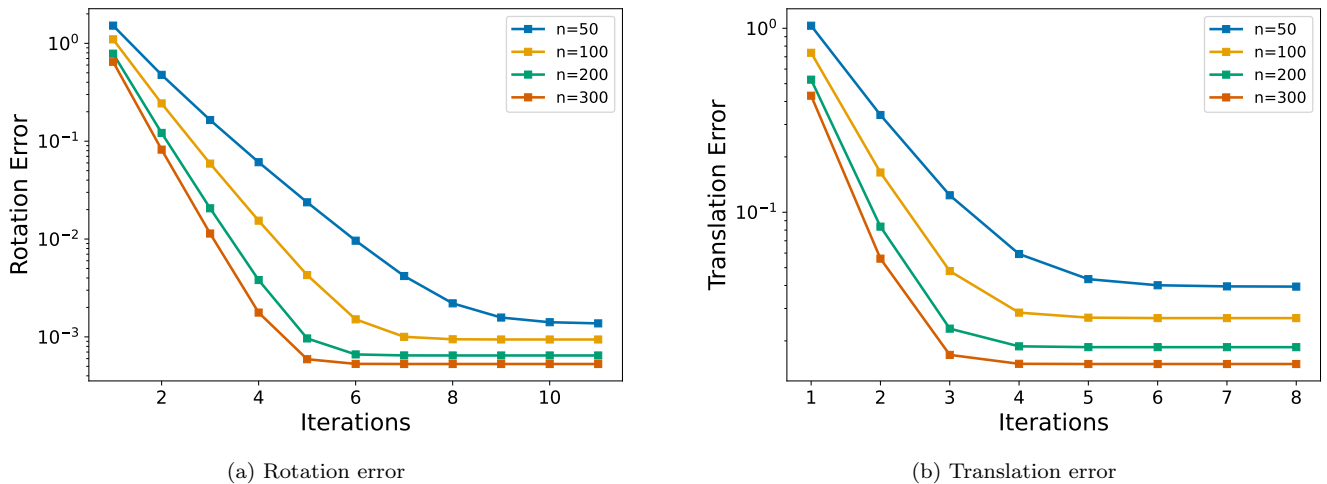


Figure 1: Error decay over iterations: (a) rotation error, (b) translation error, with $(\sigma_t, \sigma_r) = (0.1, 10^\circ)$ and $p = 0.3$.

4.3 Efficiency and Accuracy on Real Data

We evaluate our method on real data from the Stanford 3D Scanning Repository¹ and compare it against EIG and SDR methods. To construct the measurement matrix, we first use Iterative Closest Point (ICP) algorithm (Besl and McKay, 1992) to estimate relative rigid motions, on which we apply additional rigid-motion perturbation. Specifically, the rotation angle (in degrees) is sampled from $\mathcal{N}(0, 1)$, the rotation axis is drawn uniformly from the unit sphere, and the translation vector (in meters) has i.i.d. entries following $\mathcal{N}(0, 0.001^2)$, consistent with the scale of translations in the datasets. All results are averaged over 100 independent trials.

Four datasets are considered in our real-data experiments: bunny, buddha, dragon, and armadillo. Figure 2 visualizes the shapes after applying DQGPM to align and merge the corresponding point clouds.

¹<http://graphics.stanford.edu/data/3Dscanrep>

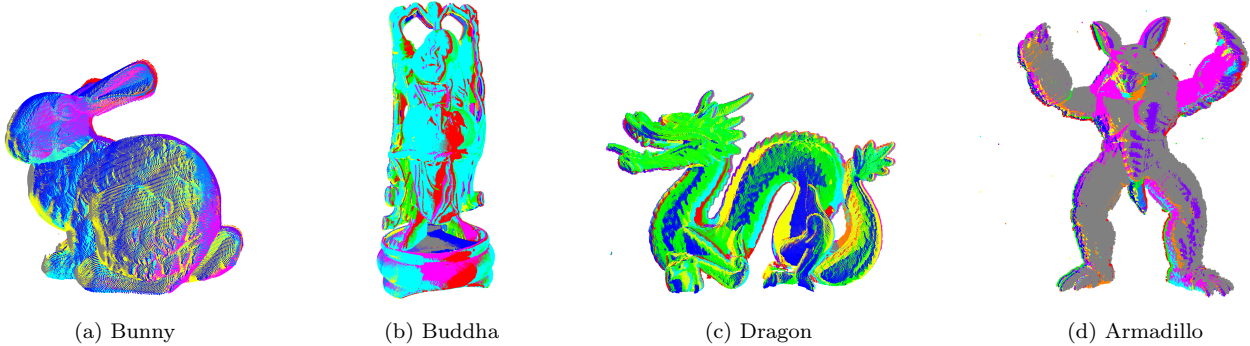


Figure 2: 3D reconstructions obtained by DQGPM on four real datasets. Colors indicate individual point clouds.

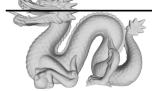
Table 4: Performance on four real datasets under $(\sigma_t, \sigma_r) = (0.001, 1^\circ)$: missing rate, time, and errors.

		BUNNY		BUDDHA		DRAGON		ARMADILLO	
		SPARSE	DENSE	SPARSE	DENSE	SPARSE	DENSE	SPARSE	DENSE
MISSING		48.00%	13.33%	66.67%	18.67%	60.44%	19.44%	58.33%	
TIME	DQGPM	0.0072	0.0023	0.0216	0.0024	0.0126	0.0027	0.0137	
	SDR	0.0954	0.0887	0.1078	0.0937	0.1226	0.1020	0.1114	
EIG	DQGPM	0.0030	0.0032	0.0036	0.0032	0.0051	0.0053	0.0071	
	SDR	0.0188	0.0192	0.0233	0.0218	0.0249	0.0198	0.0198	
ERROR_R	DQGPM	3.6349	0.1395	3.1227	0.2079	3.1307	0.5665	3.1251	
	EIG	3.4519	0.0923	3.1022	0.1704	3.1346	0.3637	3.1273	
ERROR_T	DQGPM	0.0012	0.0007	0.0016	0.0009	0.0019	0.0012	0.0013	
	SDR	0.0675	0.0014	0.0003	0.0014	0.0003	0.0013	0.0003	
EIG	DQGPM	0.0506	0.0006	0.0002	0.0009	0.0003	0.0006	0.0003	

To evaluate robustness under sparse observations, we construct two types of ICP-based measurement matrices for the last three datasets. The sparse version is obtained by running ICP without any initialization, whereas the dense version uses an initialization in which the relative orientation is inferred from the point-cloud file names. The bunny dataset only admits the sparse construction, since its file names do not encode relative orientations and therefore do not provide a meaningful ICP initializer.

Table 5 visualizes cross-sectional slices of the registered point clouds produced by different methods. Better alignment manifests as sharper, cleaner contours with fewer ghosting artifacts and outliers. Figure 3 shows the evolution of the alignment over DQGPM iterations, where the misregistration decreases monotonically and the point clouds gradually collapse to a consistent configuration. The results for estimation error and CPU time are summarized in Table 4. Overall, DQGPM attains comparable best accuracy with substantially lower runtime than SDR, while maintaining strong performance even when a large fraction of measurements is missing.

Table 5: Cross-sectional views of the aligned point clouds on four real datasets for different methods.

Dataset	DQGPM	SDR	EIG	
Buddha				
Dragon				
Armadillo				

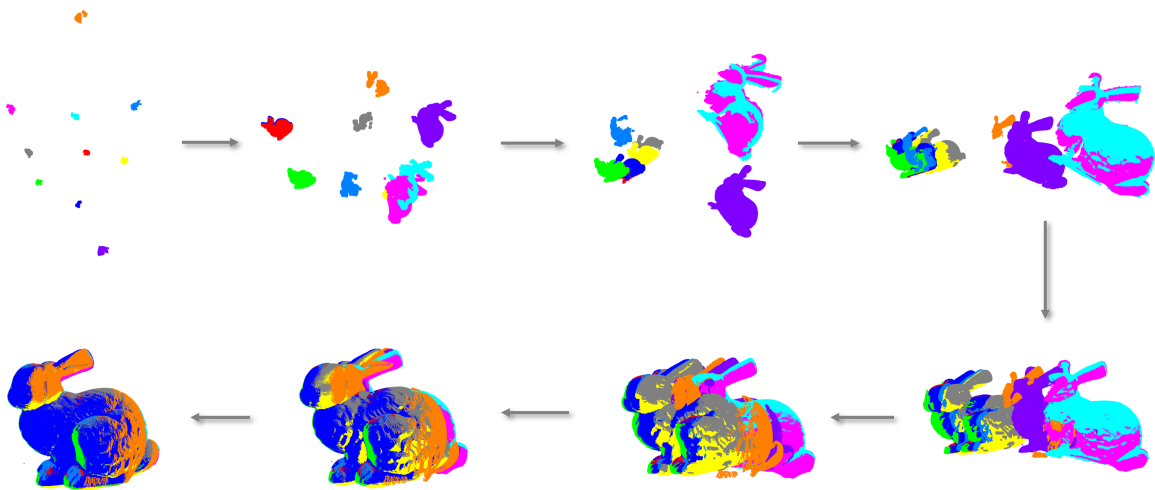


Figure 3: Point-cloud alignment over DQGPM iterations.

References

- Mica Arie-Nachimson, Shahar Z. Kovalsky, Ira Kemelmacher-Shlizerman, Amit Singer, and Ronen Basri. Global motion estimation from point matches. In *2012 Second International Conference on 3D Imaging, Modeling, Processing, Visualization & Transmission (3DIMPVT)*, pages 81–88, Zurich, Switzerland, 2012. IEEE.
- Federica Arrigoni, Beatrice Rossi, and Andrea Fusiello. Global registration of 3D point sets via LRS decomposition. In *Computer Vision – ECCV 2016*, volume 9908 of *Lecture Notes in Computer Science*, pages 489–504, Cham, 2016a. Springer.
- Federica Arrigoni, Beatrice Rossi, and Andrea Fusiello. Spectral synchronization of multiple views in $SE(3)$. *SIAM Journal on Imaging Sciences*, 9(4):1963–1990, 2016b.
- Raouf Benjemaa and Francis Schmitt. A solution for the registration of multiple 3D point sets using unit

quaternions. In Hans Burkhardt and Bernd Neumann, editors, *Computer Vision — ECCV'98*, volume 1407 of *Lecture Notes in Computer Science*, pages 34–50, Berlin, Heidelberg, 1998. Springer.

Paul J. Besl and Neil D. McKay. Method for registration of 3-D shapes. In *Sensor Fusion IV: Control Paradigms and Data Structures*, volume 1611 of *Proceedings of SPIE*, pages 586–606, Bellingham, WA, USA, 1992. SPIE.

Nicolas Boumal. Nonconvex phase synchronization. *SIAM Journal on Optimization*, 26(4):2355–2377, 2016.

Kunal N Chaudhury, Yuehaw Khoo, and Amit Singer. Global registration of multiple point clouds using semidefinite programming. *SIAM Journal on Optimization*, 25(1):468–501, 2015.

Xin Chen, Chunfeng Cui, Deren Han, and Liqun Qi. Non-convex pose graph optimization in SLAM via proximal linearized Riemannian ADMM. *arXiv preprint arXiv:2404.18560*, 2024.

Jiantong Cheng, Jonghyuk Kim, Zhenyu Jiang, and Wanfang Che. Dual quaternion-based graphical SLAM. *Robotics and Autonomous Systems*, 77:15–24, 2016.

Chunfeng Cui and Liqun Qi. A power method for computing the dominant eigenvalue of a dual quaternion Hermitian matrix. *Journal of Scientific Computing*, 100(1):21, 2024.

Konstantinos Daniilidis. Hand-eye calibration using dual quaternions. *The International Journal of Robotics Research*, 18(3):286–298, 1999.

Taosha Fan and Todd Murphy. Generalized proximal methods for pose graph optimization. In *Robotics Research: The 19th International Symposium ISRR*, volume 20, page 393. Springer Nature, 2022.

Andrea Fusiello, Umberto Castellani, Luca Ronchetti, and Vittorio Murino. Model acquisition by registration of multiple acoustic range views. In *Proceedings of the 7th European Conference on Computer Vision (ECCV)*, pages 805–819. Springer, 2002.

David J. H. Garling. *Clifford Algebras: An Introduction*. Number 78 in London Mathematical Society Student Texts. Cambridge University Press, Cambridge, UK, 2011.

Venu Madhav Govindu. Lie-algebraic averaging for globally consistent motion estimation. In *Proceedings of the 2004 IEEE Computer Society Conference on Computer Vision and Pattern Recognition (CVPR 2004)*, volume 1, pages 684–691. IEEE Computer Society, 2004.

Giorgio Grisetti, Rainer Kümmerle, Cyrill Stachniss, and Wolfram Burgard. A tutorial on graph-based SLAM. *IEEE Intelligent Transportation Systems Magazine*, 2(4):31–43, 2010.

Ido Hadi, Tamir Bendory, and Nir Sharon. SE(3) synchronization by eigenvectors of dual quaternion matrices. *Information and Inference: A Journal of the IMA*, 13(3), 2024.

Lei Han, Lan Xu, Dmytro Bobkov, Eckehard Steinbach, and Lu Fang. Real-time global registration for globally consistent RGB-D SLAM. *IEEE Transactions on Robotics*, 35(2):498–508, 2019.

Berthold K. P. Horn. Closed-form solution of absolute orientation using unit quaternions. *Journal of the Optical Society of America A*, 4(4):629–642, 1987.

Nianjuan Jiang, Zhaopeng Cui, and Ping Tan. A global linear method for camera pose registration. In *Proceedings of the IEEE International Conference on Computer Vision (ICCV)*, pages 481–488, Sydney, Australia, December 2013. IEEE.

- Xin Jin, Yang Shi, Yang Tang, and Xiaotai Wu. Event-triggered attitude consensus with absolute and relative attitude measurements. *Automatica*, 122:109245, 2020.
- Michel Journée, Yurii Nesterov, Peter Richtárik, and Rodolphe Sepulchre. Generalized power method for sparse principal component analysis. *Journal of Machine Learning Research*, 11(2), 2010.
- Chen Ling, Liqun Qi, and Hong Yan. Minimax principle for right eigenvalues of dual quaternion matrices and their generalized inverses. *arXiv preprint arXiv:2203.03161*, 2022.
- Shuyang Ling. Improved performance guarantees for orthogonal group synchronization via generalized power method. *SIAM Journal on Optimization*, 32(2):1018–1048, 2022.
- Huikang Liu, Man-Chung Yue, and Anthony Man-Cho So. On the estimation performance and convergence rate of the generalized power method for phase synchronization. *SIAM Journal on Optimization*, 27(4):2426–2446, 2017.
- Huikang Liu, Man-Chung Yue, and Anthony Man-Cho So. A unified approach to synchronization problems over subgroups of the orthogonal group. *Applied and Computational Harmonic Analysis*, 66:320–372, 2023.
- Minjie Liu, Shoudong Huang, Gamini Dissanayake, and Heng Wang. A convex optimization based approach for pose SLAM problems. In *2012 IEEE/RSJ International Conference on Intelligent Robots and Systems (IROS)*, pages 1898–1903, Vilamoura-Algarve, Portugal, October 2012. IEEE.
- Daniel Martinec and Tomáš Pajdla. Robust rotation and translation estimation in multiview reconstruction. In *2007 IEEE Conference on Computer Vision and Pattern Recognition (CVPR)*, pages 1–8, Minneapolis, MN, USA, June 2007. IEEE.
- Onur Özyesil and Amit Singer. Robust camera location estimation by convex programming. In *Proceedings of the IEEE Conference on Computer Vision and Pattern Recognition (CVPR)*, pages 2674–2683. IEEE, 2015.
- Liqun Qi, Chen Ling, and Hong Yan. Dual quaternions and dual quaternion vectors. *Communications on Applied Mathematics and Computation*, 4(4):1494–1508, 2022.
- David M Rosen, Luca Carlone, Afonso S Bandeira, and John J Leonard. SE-Sync: A certifiably correct algorithm for synchronization over the special Euclidean group. *The International Journal of Robotics Research*, 38(2-3):95–125, 2019.
- Gregory C Sharp, Sang W Lee, and David K Wehe. Multiview registration of 3D scenes by minimizing error between coordinate frames. *IEEE Transactions on Pattern Analysis and Machine Intelligence*, 26(8):1037–1050, 2004.
- Rangaprasad Arun Srivatsan, Gillian T. Rosen, D. Feroze Naina Mohamed, and Howie Choset. Estimating SE(3) elements using a dual quaternion based linear Kalman filter. In *Robotics: Science and Systems*, Ann Arbor, Michigan, USA, 2016.
- Johan Thunberg, Wenjun Song, Eduardo Montijano, Yiguang Hong, and Xiaoming Hu. Distributed attitude synchronization control of multi-agent systems with switching topologies. *Automatica*, 50(3):832–840, 2014.
- Roberto Tron and Kostas Daniilidis. Statistical pose averaging with non-isotropic and incomplete relative measurements. In David Fleet, Tomáš Pajdla, Bernt Schiele, and Tinne Tuytelaars, editors, *Computer Vision – ECCV 2014*, volume 8693 of *Lecture Notes in Computer Science*, pages 804–819. Springer, 2014.

Qian-Yi Zhou, Jaesik Park, and Vladlen Koltun. Fast global registration. In Bastian Leibe, Jiří Matas, Nicu Sebe, and Max Welling, editors, *Computer Vision – ECCV 2016*, volume 9906 of *Lecture Notes in Computer Science*, pages 766–782, Cham, 2016. Springer.

Linglingzhi Zhu, Chong Li, and Anthony Man-Cho So. Rotation group synchronization via quotient manifold. *arXiv preprint arXiv:2306.12730*, 2023.

A Algebras

A.1 Dual Numbers

We denote the set of dual numbers as \mathbb{D} . A dual number d has the form of $d = d_{st} + d_{\mathcal{I}}\epsilon$ with d_{st} and $d_{\mathcal{I}}$ in real number field. We call d_{st} the real part or standard part, and $d_{\mathcal{I}}$ is regarded as the dual part or infinitesimal part. ϵ is a dual unit satisfying $\epsilon^2 = 0$, which is commutative in multiplication with real numbers, complex numbers, and quaternion numbers. A dual number is called infinitesimal if it only has dual part, otherwise, we call it appreciable.

Addition and multiplication on dual number can be defined as follows: for $d_i \in \mathbb{D}$, where $d_i = d_{i,st} + d_{i,\mathcal{I}}\epsilon$, $i = 1, 2$, we have

$$\begin{aligned} d_1 + d_2 &= (d_{1,st} + d_{2,st}) + (d_{1,\mathcal{I}} + d_{2,\mathcal{I}})\epsilon \\ d_1 d_2 &= d_{1,st}d_{2,st} + (d_{1,st}d_{2,\mathcal{I}} + d_{1,\mathcal{I}}d_{2,st})\epsilon \end{aligned}$$

Although the above properties show the similarity between dual numbers and complex number field, we should notice that the algebra of dual numbers form a ring but not a field as infinitesimal dual number does not have an inverse element. For the dual number ring, $d = d_{st} + d_{\mathcal{I}}\epsilon \in \mathbb{D}$ with $d_{st} \neq 0$ has an inverse of

$$d^{-1} = d_{st}^{-1}(1 - d_{\mathcal{I}}d_{st}^{-1}\epsilon),$$

The zero element of \mathbb{D} is $0_{\mathbb{D}} := 0 + 0\epsilon$ and the identity element is $1_{\mathbb{D}} := 1 + 0\epsilon$. Moreover, [Qi et al. \(2022\)](#) defined the square root and absolute value of d as

$$\sqrt{d} = \sqrt{d_{st}} + \frac{d_{\mathcal{I}}}{2\sqrt{d_{st}}}\epsilon$$

and

$$|d| = \begin{cases} |d_{st}| + \text{sgn}(d_{st})d_{\mathcal{I}}\epsilon, & \text{if } d_{st} \neq 0, \\ |d_{\mathcal{I}}|\epsilon, & \text{otherwise.} \end{cases}$$

where $\text{sgn}(u) = \frac{u}{|u|}$ for nonzero real number u and $\text{sgn}(u) = 0$ otherwise. For dual numbers $x = a + b\epsilon$ and $y = c + d\epsilon$, a total order $x > y$ is given in [Qi et al. \(2022\)](#) by $a > c$ or $a = c$ and $b > d$, and $x = y$ if and only if $a = c$ and $b = d$.

A.2 Quaternions

We denote the set of quaternions by \mathbb{H} . Let $\mathbf{i}, \mathbf{j}, \mathbf{k}$ be an orthonormal basis of \mathbb{R}^3 . A quaternion $q \in \mathbb{H}$ is represented as the sum of a scalar part q_0 and a vector part $\mathbf{q} = (q_1, q_2, q_3)$, namely,

$$q = q_0 + \mathbf{q} = q_0 + q_1\mathbf{i} + q_2\mathbf{j} + q_3\mathbf{k}.$$

Equivalently, q can be written as the four-dimensional vector (q_0, q_1, q_2, q_3) . The real part of q is $\text{Re}(q) = q_0$, and the imaginary part is $\text{Im}(q) = q_1\mathbf{i} + q_2\mathbf{j} + q_3\mathbf{k}$.

Motivated by the dot product and cross product in \mathbb{R}^3 , the product of two quaternions $p = p_0 + \mathbf{p}$ and $q = q_0 + \mathbf{q}$ is given by

$$pq = p_0q_0 - \mathbf{p} \cdot \mathbf{q} + p_0\mathbf{q} + q_0\mathbf{p} + \mathbf{p} \times \mathbf{q},$$

where \mathbf{pq} denotes the dot product, i.e., the inner product of \mathbf{p} and \mathbf{q} . Quaternion multiplication satisfies the distributive law but is generally noncommutative. Consequently, the quaternion algebra forms a noncommutative division ring.

The conjugate of a quaternion $q = q_0 + q_1\mathbf{i} + q_2\mathbf{j} + q_3\mathbf{k}$ is defined as $q^* := q_0 - q_1\mathbf{i} - q_2\mathbf{j} - q_3\mathbf{k}$. Its magnitude is $|q| = \sqrt{q_0^2 + q_1^2 + q_2^2 + q_3^2}$. Consequently, the inverse of any nonzero quaternion q is given by $q^{-1} = q^*/|q|^2$. Moreover, for any two quaternions p and q , the conjugation reverses the order of multiplication, i.e., $(pq)^* = q^*p^*$. A quaternion q with $|q| = 1$ is called a unit quaternion (or a rotation quaternion).

We denote by \mathbb{H}^n the set of n -dimensional quaternion vectors. For $\mathbf{x} = (x_1, x_2, \dots, x_n)^\top$ and $\mathbf{y} = (y_1, y_2, \dots, y_n)^\top \in \mathbb{H}^n$, we define

$$\mathbf{x}^* \mathbf{y} = \sum_{i=1}^n x_i^* y_i,$$

where $\mathbf{x}^* = (x_1^*, x_2^*, \dots, x_n^*)$ denotes the conjugate transpose of \mathbf{x} .

A.3 Dual Quaternion

We denote the set of dual quaternions by \mathbb{DH} . Any dual quaternion $q \in \mathbb{DH}$ can be written as

$$q = q_{st} + q_{\mathcal{I}}\epsilon,$$

where $q_{st}, q_{\mathcal{I}} \in \mathbb{H}$ are referred to as the standard part and the dual part of q , respectively. When $q_{st} \neq 0$, the dual quaternion q is called appreciable. Moreover, if both q_{st} and $q_{\mathcal{I}}$ are imaginary quaternions, then q is called an imaginary dual quaternion.

The conjugate of q is defined by

$$q^* = q_{st}^* + q_{\mathcal{I}}^*\epsilon.$$

If $q = q^*$, then q is a dual number. If q is imaginary, then $q^* = -q$.

The magnitude of q is defined as

$$|q| := \begin{cases} |q_{st}| + \frac{(q_{st}q_{\mathcal{I}}^* + q_{\mathcal{I}}q_{st}^*)}{2|q_{st}|}\epsilon, & \text{if } q_{st} \neq 0, \\ |q_{\mathcal{I}}|\epsilon, & \text{otherwise,} \end{cases}$$

which is a dual number.

A dual quaternion q is said to be invertible if there exists a dual quaternion p such that $pq = qp = 1$. A dual quaternion q is invertible if and only if it is appreciable. In this case, its inverse is

$$q^{-1} = q_{st}^{-1} - q_{st}^{-1}q_{\mathcal{I}}q_{st}^{-1}\epsilon.$$

We denote the set of unit dual quaternions by UDQ . A dual quaternion q is called a unit dual quaternion if $|q| = 1$. Any unit dual quaternion is invertible, and its inverse coincides with its conjugate, i.e., $q^{-1} = q^*$. Moreover, q is a unit dual quaternion if and only if q_{st} is a unit quaternion and

$$q_{st}q_{\mathcal{I}}^* + q_{\mathcal{I}}q_{st}^* = q_{st}^*q_{\mathcal{I}} + q_{\mathcal{I}}^*q_{st} = 0.$$

Consider two dual quaternions $p = p_{st} + p_{\mathcal{I}}\epsilon$ and $q = q_{st} + q_{\mathcal{I}}\epsilon$. Their sum is given by

$$p + q = (p_{st} + q_{st}) + (p_{\mathcal{I}} + q_{\mathcal{I}})\epsilon,$$

and their product is

$$pq = p_{st}q_{st} + (p_{st}q_{\mathcal{I}} + p_{\mathcal{I}}q_{st})\epsilon.$$

Denote the set of n -dimensional dual quaternion vectors by \mathbb{DH}^n . For $\mathbf{x} = (x_1, x_2, \dots, x_n)$, the 2-norm is defined as

$$\|\mathbf{x}\|_2 := \begin{cases} \sqrt{\sum_{i=1}^n |x_i|^2}, & \mathbf{x}_{st} \neq \mathbf{0}_n, \\ \sqrt{\sum_{i=1}^n |(x_i)_{\mathcal{I}}|^2} \epsilon, & \text{otherwise.} \end{cases}$$

B Representation of $\text{SO}(3)$ and $\text{SE}(3)$

Let $\mathbf{R} \in \text{SO}(3)$ be a rotation element and a point \mathbf{v} under rotation \mathbf{R} has the form of $\mathbf{R}\mathbf{v}$, Proposition B.1 implies that $q\mathbf{v}q^*$ is a pure quaternion with the form of $0 + \mathbf{R}\mathbf{v}$. It gives a result for representing $\text{SO}(3)$ element with unit quaternion (Garling, 2011, Sec. 4.9), which shows that quaternions can be used to obtain double cover of $\text{SO}(3)$ group. More specifically, $\psi : \mathbb{UQ} \rightarrow \text{SO}(3)$ is a 2-to-1 surjective group homomorphism of \mathbb{UQ} onto $\text{SO}(3)$ with kernel $\{1, -1\}$, such that $\psi^{-1}(\mathbf{R}) = \{q, -q\}$ for every $\mathbf{R} \in \text{SO}(3)$.

Proposition B.1 (Horn (1987, Sec. 3)). *For any unit quaternion with a representation of*

$$q = q_0 + \mathbf{q}_{\mathbf{R}} = \cos \frac{\theta}{2} + \hat{\mathbf{u}} \sin \frac{\theta}{2}, \quad (\text{B.1})$$

a rotation of random vector $\mathbf{v}_{\mathbf{R}} \in \mathbb{R}^3$ about an axis (denoted by unit vector $\hat{\mathbf{u}} \in \mathbb{R}^3$) by an angle θ can be represented by the operator

$$\psi_q(\mathbf{v}_{\mathbf{R}}) = q\mathbf{v}q^*,$$

where \mathbf{v} is treated as a quaternion with scalar part 0 and vector part $\mathbf{v}_{\mathbf{R}}$.

Let $(\mathbf{R}, \mathbf{t}) \in \text{SE}(3)$ represents an element of rigid motion with rotation $\mathbf{R} \in \text{SO}(3)$ and translation $\mathbf{t} \in \mathbb{R}^3$. Consider a rigid line ℓ in the Plücker coordinates $(\hat{\mathbf{l}}, \mathbf{m})$. Similar to the quaternion and $\text{SO}(3)$ case in the above subsection, a correspondence between $\text{SE}(3)$ and unit dual quaternion can be constructed. To be operated on by dual quaternion, the line ℓ needs to be converted into a dual quaternion form $\ell = \hat{\mathbf{l}} + \epsilon \mathbf{m}$. The transformation operator is given by a unit dual quaternion which contains information of rotation and translation at the same time.

Proposition B.2 (Daniilidis (1999, Sec. 3)). *Let $\ell_i = \hat{\mathbf{l}}_i + \epsilon \mathbf{m}_i, i = 1, 2$ be the dual quaternion describing of line ℓ_i , line ℓ_1 is transformed into line ℓ_2 with a rotation $R \in \text{SO}(3)$ followed by a translation $\mathbf{t} \in \mathbb{R}^3$. Then*

$$\ell_2 = \phi_x(\ell_1) = x\ell_1x^*,$$

where x is a unit dual quaternion in the form of

$$x = \left(1 + \frac{\epsilon}{2}\mathbf{t}\right)q, \quad (\text{B.2})$$

with q being the unit quaternion representation of R following the rule in Proposition B.1 and $\mathbf{t} \in \mathbb{R}^3$ being the translation vector.

Proposition B.2 offers an approach to represent elements in $\text{SE}(3)$ in nearly the same way as we represent element in $\text{SO}(3)$ by quaternions, where $(\mathbf{R}, \mathbf{t}) \in \text{SE}(3)$ is described by $x = (1 + \frac{\epsilon}{2}\mathbf{t})q \in \text{UDQ}$. ϕ can also be described as a 2-to-1 surjective group homomorphism from UDQ to $\text{SE}(3)$, such that $\phi^{-1}(\mathbf{R}, \mathbf{t}) = \{-x, x\}$ for all $(\mathbf{R}, \mathbf{t}) \in \text{SE}(3)$. Particularly, when $\mathbf{t} = 0$, x becomes a pure quaternion q and the $\text{SE}(3)$ element degenerate into a $\text{SO}(3)$ element accordingly. This shows a special case for Proposition B.2, which is consistent with Proposition B.1. We will focus on studying the synchronization problem on $\text{SE}(3)$ case in the whole work, and this can also cover results in $\text{SO}(3)$ by a degeneration of $\text{SE}(3)$ elements.

C Proofs in Section 2

C.1 Proof of Proposition 2.1

For any $\mathbf{x} \in \text{UDQ}^n$, let $\mathbf{X} := \mathbf{x}\mathbf{x}^*$. Using $\|\mathbf{A}\|_F^2 = \text{tr}(\mathbf{A}\mathbf{A}^*)$ and $\mathbf{C}^* = \mathbf{C}$ (Hermitian),

$$\|\mathbf{C} - \mathbf{X}\|_F^2 = \text{tr}((\mathbf{C} - \mathbf{X})(\mathbf{C} - \mathbf{X})^*) = \text{tr}(\mathbf{C}^2) - \text{tr}(\mathbf{C}\mathbf{X} + \mathbf{X}\mathbf{C}) + \text{tr}(\mathbf{X}^2).$$

Moreover, $\mathbf{X}^2 = \mathbf{x}\mathbf{x}^*\mathbf{x}\mathbf{x}^* = \mathbf{x}(\mathbf{x}^*\mathbf{x})\mathbf{x}^* = n\mathbf{X}$ and $\text{tr}(\mathbf{X}) = \sum_{i=1}^n |\mathbf{x}_i|^2 = \mathbf{x}^*\mathbf{x} = n$, hence $\text{tr}(\mathbf{X}^2) = n^2$. Therefore, minimizing $\|\mathbf{C} - \mathbf{x}\mathbf{x}^*\|_F^2$ is equivalent to maximizing $\text{tr}(\mathbf{C}\mathbf{X} + \mathbf{X}\mathbf{C})$.

By the unitary decomposition of Hermitian dual quaternion matrices, $\mathbf{X} = \mathbf{U}\boldsymbol{\Sigma}\mathbf{U}^*$ with $\boldsymbol{\Sigma} = \text{diag}(n, 0, \dots, 0)$ and the first column of \mathbf{U} equal to $\mathbf{u}_1 = \mathbf{x}/\sqrt{n}$ (cf. (Qi et al., 2022, Theorem 4.1)). Let $\mathbf{Y} := \mathbf{U}^*\mathbf{C}\mathbf{U} = (y_{ij})$. Using invariance of the (scalar/dual-number) trace under unitary similarity,

$$\text{tr}(\mathbf{C}\mathbf{X} + \mathbf{X}\mathbf{C}) = \text{tr}(\mathbf{U}(\boldsymbol{\Sigma}\mathbf{Y} + \mathbf{Y}\boldsymbol{\Sigma})\mathbf{U}^*) = \text{tr}(\boldsymbol{\Sigma}\mathbf{Y} + \mathbf{Y}\boldsymbol{\Sigma}) = 2n \cdot y_{11}.$$

Since $y_{11} = \mathbf{u}_1^*\mathbf{C}\mathbf{u}_1 = (\mathbf{x}^*\mathbf{C}\mathbf{x})/n$, we obtain $\text{tr}(\mathbf{C}\mathbf{X} + \mathbf{X}\mathbf{C}) = 2\mathbf{x}^*\mathbf{C}\mathbf{x}$. Hence, the argmin of (2.1) equals the argmax of (P), and the optimal values differ only by a factor of 2.

C.2 Proof of Proposition 2.4

Let

$$\hat{z} := \arg \min_{z \in \text{UDQ}} \|\mathbf{x} - \hat{\mathbf{x}}z\|_2.$$

Expanding the square and using $\|\mathbf{x}\|_2^2 = \|\hat{\mathbf{x}}\|_2^2 = n$ and $\|\hat{\mathbf{x}}z\|_2 = \|\hat{\mathbf{x}}\|_2$ for all $z \in \text{UDQ}$,

$$\|\mathbf{x} - \hat{\mathbf{x}}z\|_2^2 = \|\mathbf{x}\|_2^2 + \|\hat{\mathbf{x}}z\|_2^2 - (\mathbf{x}^*\hat{\mathbf{x}}z + (\mathbf{x}^*\hat{\mathbf{x}}z)^*) = 2n - (z^*\hat{\mathbf{x}}^*\mathbf{x} + (z^*\hat{\mathbf{x}}^*\mathbf{x})^*).$$

Hence,

$$\hat{z} = \arg \min_{z \in \text{UDQ}} \|\mathbf{x} - \hat{\mathbf{x}}z\|_2 = \arg \max_{z \in \text{UDQ}} (z^*\hat{\mathbf{x}}^*\mathbf{x} + (z^*\hat{\mathbf{x}}^*\mathbf{x})^*). \quad (\text{C.1})$$

Write $\hat{z}^* = c + d\epsilon$ and $\hat{\mathbf{x}}^*\mathbf{x} = a + b\epsilon$ with $c, d, a, b \in \mathbb{H}$. Since $\hat{z} \in \text{UDQ}$, we have

$$c^*c = 1,$$

$$dc^* + cd^* = 0.$$

Moreover,

$$z^*\hat{\mathbf{x}}^*\mathbf{x} + (z^*\hat{\mathbf{x}}^*\mathbf{x})^* = ca + a^*c^* + (cb + b^*c^* + da + a^*d^*)\epsilon,$$

and thus (C.1) is equivalent to

$$\begin{aligned} \max_{c, d \in \mathbb{H}} \quad & ca + a^*c^* + (cb + b^*c^* + da + a^*d^*)\epsilon \\ \text{s.t.} \quad & dc^* + cd^* = 0, \quad c^*c = 1. \end{aligned}$$

Since the objective is a dual number and comparisons are made lexicographically (first by the primal part, then by the dual part), we consider first the primal (rotation) part:

$$\max_{c \in \mathbb{H}} \quad ca + a^*c^* \quad \text{s.t.} \quad c^*c = 1.$$

If $a \neq 0$, the maximizer is

$$c = \frac{a^*}{|a|}.$$

If $a = 0$, then $ca + a^*c^* = 0$ for all unit c , hence any c with $c^*c = 1$ is optimal (the maximizer is not unique). In either case, letting

$$p := \max_{z \in \text{UDQ}} z^* \hat{\mathbf{x}}^* \mathbf{x},$$

we have (by the definition of the dual quaternion modulus)

$$\max_{z \in \text{UDQ}} (z^* \hat{\mathbf{x}}^* \mathbf{x} + (z^* \hat{\mathbf{x}}^* \mathbf{x})^*) = p + p^* = 2|\hat{\mathbf{x}}^* \mathbf{x}|.$$

Plugging this into (C.1) yields

$$d^2(\hat{\mathbf{x}}, \mathbf{x}) = \min_{z \in \text{UDQ}} \|\mathbf{x} - \hat{\mathbf{x}}z\|_2^2 = 2n - 2|\hat{\mathbf{x}}^* \mathbf{x}|. \quad (\text{C.3})$$

In addition,

$$\begin{aligned} \mathbf{x}^* \hat{\mathbf{x}} \hat{\mathbf{x}}^* \mathbf{x} &\leq |\mathbf{x}^* \hat{\mathbf{x}} \hat{\mathbf{x}}^* \mathbf{x}| = |\langle \mathbf{x}, \hat{\mathbf{x}} \hat{\mathbf{x}}^* \mathbf{x} \rangle| \leq \|\mathbf{x}\|_2 \|\hat{\mathbf{x}} \hat{\mathbf{x}}^* \mathbf{x}\|_2 \\ &= \sqrt{n} \|\hat{\mathbf{x}}\|_2 |\hat{\mathbf{x}}^* \mathbf{x}| = n |\hat{\mathbf{x}}^* \mathbf{x}|. \end{aligned} \quad (\text{C.4})$$

Here, $\mathbf{x}^* \hat{\mathbf{x}} \hat{\mathbf{x}}^* \mathbf{x} = |\hat{\mathbf{x}}^* \mathbf{x}|^2$ is a dual number and hence admits a total order. The first inequality follows from Qi et al. (2022, Theorem 2), and the second from the Cauchy–Schwarz inequality (Ling et al., 2022, Proposition 4.7). Therefore,

$$|\hat{\mathbf{x}}^* \mathbf{x}| \geq \frac{1}{n} \mathbf{x}^* \hat{\mathbf{x}} \hat{\mathbf{x}}^* \mathbf{x} \implies d^2(\hat{\mathbf{x}}, \mathbf{x}) = 2n - 2|\hat{\mathbf{x}}^* \mathbf{x}| \leq \frac{1}{n} (2n^2 - 2\mathbf{x}^* \hat{\mathbf{x}} \hat{\mathbf{x}}^* \mathbf{x}).$$

Recall that $\mathbf{C} = \hat{\mathbf{x}} \hat{\mathbf{x}}^* + \Delta$. Then

$$\begin{aligned} 2n^2 - 2\mathbf{x}^* \hat{\mathbf{x}} \hat{\mathbf{x}}^* \mathbf{x} &= 2\hat{\mathbf{x}}^* \hat{\mathbf{x}} \hat{\mathbf{x}}^* \hat{\mathbf{x}} - 2\mathbf{x}^* \hat{\mathbf{x}} \hat{\mathbf{x}}^* \mathbf{x} \\ &= 2\hat{\mathbf{x}}^* (\mathbf{C} - \Delta) \hat{\mathbf{x}} - 2\mathbf{x}^* (\mathbf{C} - \Delta) \mathbf{x} \\ &\leq 2\mathbf{x}^* \Delta \mathbf{x} - 2\hat{\mathbf{x}}^* \Delta \hat{\mathbf{x}} \\ &= (\mathbf{x} + \hat{\mathbf{x}})^* \Delta (\mathbf{x} - \hat{\mathbf{x}}) + (\mathbf{x} - \hat{\mathbf{x}})^* \Delta (\mathbf{x} + \hat{\mathbf{x}}), \end{aligned}$$

where the inequality uses the assumption $\mathbf{x}^* \mathbf{C} \mathbf{x} \geq \hat{\mathbf{x}}^* \mathbf{C} \hat{\mathbf{x}}$. Combining the above display with (C.3)–(C.4) gives

$$d^2(\hat{\mathbf{x}}, \mathbf{x}) \leq \frac{1}{n} \left[(\mathbf{x} + \hat{\mathbf{x}})^* \Delta (\mathbf{x} - \hat{\mathbf{x}}) + (\mathbf{x} - \hat{\mathbf{x}})^* \Delta (\mathbf{x} + \hat{\mathbf{x}}) \right] \leq \frac{2}{n} |(\mathbf{x} + \hat{\mathbf{x}})^* \Delta (\mathbf{x} - \hat{\mathbf{x}})|.$$

Using the Cauchy–Schwarz inequality and the definition of the induced operator norm, for any compatible \mathbf{u}, \mathbf{v} we have $|\mathbf{u}^* \Delta \mathbf{v}| \leq \|\mathbf{u}\|_2 \|\Delta\|_{\text{op}} \|\mathbf{v}\|_2$. Therefore,

$$d^2(\hat{\mathbf{x}}, \mathbf{x}) \leq \frac{2}{n} \|\mathbf{x} + \hat{\mathbf{x}}\|_2 \|\Delta\|_{\text{op}} \|\mathbf{x} - \hat{\mathbf{x}}\|_2.$$

Finally, by right-multiplying \mathbf{x} with the optimal aligner $\hat{\mathbf{z}}$ (which does not change the hypothesis $\mathbf{x}^* \mathbf{C} \mathbf{x} \geq \hat{\mathbf{x}}^* \mathbf{C} \hat{\mathbf{x}}$ nor the value of $d(\hat{\mathbf{x}}, \mathbf{x})$), we may assume $d(\hat{\mathbf{x}}, \mathbf{x}) = \|\mathbf{x} - \hat{\mathbf{x}}\|_2$. Then $\|\mathbf{x} + \hat{\mathbf{x}}\|_2 \leq \|\mathbf{x}\|_2 + \|\hat{\mathbf{x}}\|_2 = 2\sqrt{n}$ and

$$d^2(\hat{\mathbf{x}}, \mathbf{x}) \leq \frac{2}{n} \cdot 2\sqrt{n} \|\Delta\|_{\text{op}} d(\hat{\mathbf{x}}, \mathbf{x}) = \frac{4}{\sqrt{n}} \|\Delta\|_{\text{op}} d(\hat{\mathbf{x}}, \mathbf{x}),$$

which implies $d(\hat{\mathbf{x}}, \mathbf{x}) \leq \frac{4}{\sqrt{n}} \|\Delta\|_{\text{op}}$. This completes the proof.

C.3 Proof of Lemma 2.5

Let $u := \mathcal{N}(y) \in \text{UDQ}$, and write

$$y = y_{st} + y_{\mathcal{I}}\epsilon, \quad z = z_{st} + z_{\mathcal{I}}\epsilon, \quad u = u_{st} + u_{\mathcal{I}}\epsilon,$$

with $y_{st}, y_{\mathcal{I}}, z_{st}, z_{\mathcal{I}}, u_{st}, u_{\mathcal{I}} \in \mathbb{H}$. Recall that for any dual quaternion $q = q_{st} + q_{\mathcal{I}}\epsilon$,

$$|q|^2 = qq^* = |q_{st}|^2 + 2\epsilon \text{sc}(q_{st}q_{\mathcal{I}}^*),$$

which is a nonnegative dual number; hence it admits a total order, and it suffices to prove $|u - z|^2 \leq 4|y - z|^2$.

Step 1: Expand $|u - z|^2$. Since $u, z \in \text{UDQ}$, we have $|u_{st}| = |z_{st}| = 1$ and $\text{sc}(u_{st}u_{\mathcal{I}}^*) = \text{sc}(z_{st}z_{\mathcal{I}}^*) = 0$. Thus,

$$\begin{aligned} |u - z|^2 &= |(u_{st} - z_{st}) + (u_{\mathcal{I}} - z_{\mathcal{I}})\epsilon|^2 \\ &= |u_{st} - z_{st}|^2 + 2\epsilon \text{sc}((u_{st} - z_{st})(u_{\mathcal{I}} - z_{\mathcal{I}})^*) \\ &= (2 - 2\text{sc}(u_{st}z_{st}^*)) - 2\epsilon(\text{sc}(u_{st}z_{\mathcal{I}}^*) + \text{sc}(z_{st}u_{\mathcal{I}}^*)). \end{aligned}$$

Step 2: Expand $4|y - z|^2$. Similarly,

$$\begin{aligned} 4|y - z|^2 &= 4|(y_{st} - z_{st}) + (y_{\mathcal{I}} - z_{\mathcal{I}})\epsilon|^2 \\ &= 4|y_{st} - z_{st}|^2 + 8\epsilon \text{sc}((y_{st} - z_{st})(y_{\mathcal{I}} - z_{\mathcal{I}})^*) \\ &= 4(|y_{st}|^2 + 1 - 2\text{sc}(y_{st}z_{st}^*)) + 8\epsilon(\text{sc}(y_{st}y_{\mathcal{I}}^*) - \text{sc}(y_{st}z_{\mathcal{I}}^*) - \text{sc}(z_{st}y_{\mathcal{I}}^*)), \end{aligned}$$

where we used $\text{sc}(z_{st}z_{\mathcal{I}}^*) = 0$ for $z \in \text{UDQ}$.

Step 3: Compare the standard parts.

Case 1: $y_{st} \neq 0$. By the definition of \mathcal{N} , we have $u_{st} = y_{st}/|y_{st}|$. Let $r := |y_{st}| > 0$ and $s := \text{sc}(y_{st}z_{st}^*)$. Note that $|z_{st}| = 1$ and $|\text{sc}(y_{st}z_{st}^*)| \leq |y_{st}z_{st}^*| = |y_{st}| = r$, hence $s \in [-r, r]$. Moreover,

$$\text{sc}(u_{st}z_{st}^*) = \text{sc}\left(\frac{y_{st}}{r}z_{st}^*\right) = \frac{s}{r}.$$

Therefore, the standard parts satisfy

$$\begin{aligned} (|u - z|^2)_{st} &= 2 - 2\frac{s}{r}, \\ (4|y - z|^2)_{st} &= 4(r^2 + 1 - 2s) = 4r^2 + 4 - 8s. \end{aligned}$$

We claim that for all $r > 0$ and $s \in [-r, r]$,

$$2 - 2\frac{s}{r} \leq 4r^2 + 4 - 8s. \quad (\text{C.5})$$

Indeed, set $t := s/r \in [-1, 1]$. Then (C.5) is equivalent to

$$0 \leq 4r^2 + 2 + t(2 - 8r).$$

If $r \leq \frac{1}{4}$, then $2 - 8r \geq 0$ and the right-hand side is minimized at $t = -1$, giving $4r^2 + 2 - (2 - 8r) = 4r^2 + 8r \geq 0$. If $r \geq \frac{1}{4}$, then $2 - 8r \leq 0$ and the right-hand side is minimized at $t = 1$, giving $4r^2 + 2 + (2 - 8r) = 4(r - 1)^2 \geq 0$. This proves (C.5). Moreover, equality can only occur when $r = 1$ and $t = 1$, i.e., $|y_{st}| = 1$ and $\text{sc}(y_{st}z_{st}^*) = 1$, which implies $y_{st}z_{st}^* = 1$ and hence $u_{st} = y_{st} = z_{st}$.

Case 2: $y_{st} = 0$. In this case $(4|y - z|^2)_{st} = 4$. By the definition of Π , we know $u_{st} = y_{\mathcal{I}}/|y_{\mathcal{I}}|$ and $|u_{st}| = 1$. Since z_{st} is also unit, we have $\text{sc}(u_{st}z_{st}^*) \geq -1$, and thus

$$(|u - z|^2)_{st} = 2 - 2\text{sc}(u_{st}z_{st}^*) \leq 4 = (4|y - z|^2)_{st}.$$

Step 4: Conclude the dual-number inequality. Since $|u - z|^2$ and $4|y - z|^2$ are dual numbers and the order is lexicographic (standard part first), the standard-part comparison implies $|u - z|^2 \leq 4|y - z|^2$ whenever the standard inequality is strict. In the only equality case from Case 1 (namely $u_{st} = z_{st}$), we have $u - z = (u_{\mathcal{I}} - z_{\mathcal{I}})\epsilon$, hence $|u - z|^2 = 0$, and also $y_{st} = z_{st}$ implies $|y - z|^2 = 0$. Thus the inequality still holds.

Finally, since both sides are nonnegative dual numbers, taking square roots preserves the order and yields $|u - z| \leq 2|y - z|$.

C.4 Proof of Proposition 2.7

Consider any $\mathbf{u} \in \text{UDQ}^n$. If $\mathbf{y} \neq \mathbf{0}$, let $\mathcal{I} := \{i : y_i \neq 0\}$. For $i \in \mathcal{I}$, Remark 2.6 has shown that $\mathcal{N}(y_i) = \Pi(y_i)$, then

$$|\tilde{y}_i - y_i| = |\Pi(y_i) - y_i| \leq |u_i - y_i|.$$

For $i \notin \mathcal{I}$,

$$|\tilde{y}_i - y_i| = |\mathcal{N}(\mathbf{e}^* \mathbf{y}) - 0| = 1 = |u_i - y_i|.$$

If $\mathbf{y} = \mathbf{0}$,

$$\|\tilde{\mathbf{y}} - \mathbf{y}\|_2^2 = \|\mathbf{1} - \mathbf{0}\|_2^2 = n = \|\mathbf{u}\|_2^2 = \|\mathbf{u} - \mathbf{y}\|_2^2.$$

Hence,

$$\|\tilde{\mathbf{y}} - \mathbf{y}\|_2^2 = \sum_{i \notin \mathcal{I}} |\tilde{y}_i - y_i|^2 + \sum_{i \in \mathcal{I}} |\tilde{y}_i - y_i|^2 \leq \|\mathbf{u} - \mathbf{y}\|_2^2$$

for any $\mathbf{u} \in \text{UDQ}^n$, which shows $\tilde{\mathbf{y}} = \Pi(\mathbf{y})$.

C.5 Proof of Theorem 2.8

Let \mathbf{x} be a dominant right eigenvector of \mathbf{C} scaled such that $\|\mathbf{x}\|_2^2 = n$. Since \mathbf{x} is defined up to a global right multiplication by any $z \in \text{UDQ}$, we may choose $z_{\star} \in \text{UDQ}$ attaining the minimum in the definition of $d(\mathbf{x}, \hat{\mathbf{x}})$ and replace $\mathbf{x} \leftarrow \mathbf{x}z_{\star}$, so that

$$\|\mathbf{x} - \hat{\mathbf{x}}\|_2 = d(\mathbf{x}, \hat{\mathbf{x}}).$$

Define $\tilde{\mathbf{x}} = \Pi(\mathbf{x})$ as in (2.3). Then

$$d(\tilde{\mathbf{x}}, \hat{\mathbf{x}}) = \min_{z \in \text{UDQ}} \|\tilde{\mathbf{x}} - \hat{\mathbf{x}}z\|_2 \leq \|\tilde{\mathbf{x}} - \hat{\mathbf{x}}\|_2.$$

Let $\mathcal{I} := \{i : x_i \neq 0\}$,

$$\begin{aligned} \|\Pi(\mathbf{x}) - \hat{\mathbf{x}}\|_2^2 &= \sum_{i \in \mathcal{I}} |\mathcal{N}(x_i) - \hat{x}_i|^2 + \sum_{i \notin \mathcal{I}} |\mathcal{N}(\mathbf{e}^* \mathbf{x}) - \hat{x}_i|^2 \\ &\leq \sum_{i \in \mathcal{I}} 4|x_i - \hat{x}_i|^2 + 4(n - |\mathcal{I}|) \\ &= \sum_{i \in \mathcal{I}} 4|x_i - \hat{x}_i|^2 + \sum_{i \notin \mathcal{I}} 4|x_i - \hat{x}_i|^2 \\ &= 4\|\mathbf{x} - \hat{\mathbf{x}}\|_2^2, \end{aligned}$$

where the second last equality holds from

$$n - |\mathcal{I}| = \sum_{i \notin \mathcal{I}} |\hat{\mathbf{x}}_i|^2 = \sum_{i \notin \mathcal{I}} |\mathbf{x}_i - \hat{\mathbf{x}}_i|^2.$$

Next, using Lemma 2.5 componentwise and summing over $i = 1, \dots, n$, we obtain

$$\|\Pi(\mathbf{x}) - \hat{\mathbf{x}}\|_2^2 = \sum_{i=1}^n |\Pi(\mathbf{x}_i) - \hat{\mathbf{x}}_i|^2 \leq \sum_{i=1}^n 4|\mathbf{x}_i - \hat{\mathbf{x}}_i|^2 = 4\|\mathbf{x} - \hat{\mathbf{x}}\|_2^2,$$

hence $\|\tilde{\mathbf{x}} - \hat{\mathbf{x}}\|_2 \leq 2\|\mathbf{x} - \hat{\mathbf{x}}\|_2$. Therefore,

$$d(\tilde{\mathbf{x}}, \hat{\mathbf{x}}) \leq \|\tilde{\mathbf{x}} - \hat{\mathbf{x}}\|_2 \leq 2\|\mathbf{x} - \hat{\mathbf{x}}\|_2 = 2d(\mathbf{x}, \hat{\mathbf{x}}) \leq 2 \cdot \frac{4\|\Delta\|_{\text{op}}}{\sqrt{n}} = \frac{8\|\Delta\|_{\text{op}}}{\sqrt{n}},$$

where the last inequality follows from Proposition 2.4.

D Proof of Theorem 3.2

The proof for Theorem 3.2 is closely based on the following results.

Lemma D.1. *For any $\mathbf{y} \in \mathbb{DH}^n$ and any real scalar $a > 0$, the projection $\Pi(\cdot)$ onto UDQ^n satisfies*

$$\Pi(a\mathbf{y}) = \Pi(\mathbf{y}).$$

This result implies that $\Pi(\cdot)$ depends only on the direction of its argument, not its magnitude. Thus, scaling the input by a positive real scalar leaves the projection unchanged.

Lemma D.2. *For any $\mathbf{x}, \mathbf{y} \in \mathbb{DH}^n$, we have*

$$\|\Pi(\mathbf{x} + \Pi(\mathbf{x}) + \mathbf{y}) - \Pi(\mathbf{x})\|_2 \leq 2\|\mathbf{y}\|_2.$$

This lemma can be regarded as a analogical version of Lemma 2 given in Liu et al. (2023). Although some slight differences were demonstrated by the unit dual quaternion set, we can still use a semblable way to give the proof here. As an extension of Lemma D.2, we have

Lemma D.3. *For any $\mathbf{p}, \mathbf{q} \in \mathbb{DH}^n$ and $\mathbf{r} \in \text{UDQ}^n$, we have*

$$\|\Pi(\mathbf{p} + \mathbf{q}) - \mathbf{r}\|_2 \leq 2\|\mathbf{q} - \mathbf{r}\|_2 + 3\|\Pi(\mathbf{p}) - \mathbf{r}\|_2. \quad (\text{D.1})$$

By letting $p = cr$ for $c \in \mathbb{R}_{++}$ in (D.1), and forcing c to zero, we can find that Lemma D.3 becomes

$$\|\Pi(\mathbf{q}) - \mathbf{r}\|_2 \leq 2\|\mathbf{q} - \mathbf{r}\|_2,$$

which coincides with the result in Lemma 2.5. Lastly, to give a full picture of the proof for Theorem 3.2, we introduce the following lemma that demonstrates geometric properties of UDQ^n .

Lemma D.4. *For any $\mathbf{x}^k \in \text{UDQ}^n$, there exists an optimizer*

$$z_k \in \operatorname{argmin}_{z \in \text{UDQ}} \|\mathbf{x}^k - \hat{\mathbf{x}}z\|_2, \quad (\text{D.2})$$

we have

$$|\hat{\mathbf{x}}^* \mathbf{x}^k - n z_k| = \frac{1}{2} d(\mathbf{x}^k, \hat{\mathbf{x}})^2.$$

The right hand side of (D.2) is the squared distance between \mathbf{x}^k and $\hat{\mathbf{x}}$ after alignment, thus Lemma D.4 can be interpreted as an error bound condition. This lemma implies that sequence $\{\mathbf{x}^{(k)}\}_{k \geq 0}$ generated by GPM also satisfies an error bound condition, which plays an important role in proving Theorem 3.2 by bounding estimation error with distance terms. Additionally, as a degenerated case for $\text{SE}(3)$, elements in $\text{SO}(3)$ represented by unit dual quaternions with zero infinitesimal part should also satisfy (D.2). This extension on $\text{SO}(3)$ meets the error bound attained for $\text{SO}(d)$ in Liu et al. (2023), but (D.2) is tighter for $\text{SO}(3)$ case since the equality always holds.

Proof of Theorem 3.2. For each k , select $z_k \in \arg \min_{z \in \text{UDQ}} \|\mathbf{x}^k - \hat{\mathbf{x}}z\|_2$ such that Lemma D.4 holds (such a minimizer exists by Lemma D.4). Then

$$d(\mathbf{x}^{k+1}, \hat{\mathbf{x}}) = \|\mathbf{x}^{k+1} - \hat{\mathbf{x}}z_{k+1}\|_2 \leq \|\mathbf{x}^{k+1} - \hat{\mathbf{x}}z_k\|_2 = \left\| \Pi \left(\frac{2}{n} \mathbf{C} \mathbf{x}^k \right) - \hat{\mathbf{x}}z_k \right\|_2,$$

where the last equality holds from Lemma D.1. Using Lemma D.3 with

$$\mathbf{q} = \hat{\mathbf{x}}z_k + 2 \left[\frac{1}{n} (\mathbf{C} - \Delta) \mathbf{x}^k - \hat{\mathbf{x}}z_k \right] + \frac{2}{n} \Delta (\mathbf{x}^k - \hat{\mathbf{x}}z_k), \quad \mathbf{p} = \hat{\mathbf{x}}z_k + \frac{2}{n} \Delta \hat{\mathbf{x}}z_k, \quad \mathbf{r} = \hat{\mathbf{x}}z_k,$$

(note that $\mathbf{p} + \mathbf{q} = \frac{2}{n} \mathbf{C} \mathbf{x}^k$), we obtain

$$\begin{aligned} \left\| \Pi \left(\frac{2}{n} \mathbf{C} \mathbf{x}^k \right) - \hat{\mathbf{x}}z_k \right\|_2 &\leq 4 \left\| \frac{1}{n} (\mathbf{C} - \Delta) \mathbf{x}^k - \hat{\mathbf{x}}z_k + \frac{1}{n} \Delta (\mathbf{x}^k - \hat{\mathbf{x}}z_k) \right\|_2 + 3 \|\Pi(\mathbf{p}) - \mathbf{r}\|_2 \\ &\leq \frac{4}{n} \|(\mathbf{C} - \Delta) \mathbf{x}^k - n \hat{\mathbf{x}}z_k\|_2 + \frac{4}{n} \|\Delta (\mathbf{x}^k - \hat{\mathbf{x}}z_k)\|_2 + 3 \|\Pi(\mathbf{p}) - \mathbf{r}\|_2. \end{aligned}$$

For the first term, since $\mathbf{C} - \Delta = \hat{\mathbf{x}}\hat{\mathbf{x}}^*$ and $\|\hat{\mathbf{x}}\|_2 = \sqrt{n}$, Lemma D.4 yields

$$\|(\mathbf{C} - \Delta) \mathbf{x}^k - n \hat{\mathbf{x}}z_k\|_2 = \|\hat{\mathbf{x}}\|_2 |\hat{\mathbf{x}}^* \mathbf{x}^k - nz_k| = \frac{\sqrt{n}}{2} \|\mathbf{x}^k - \hat{\mathbf{x}}z_k\|_2^2.$$

For the second term, by the definition of operator norm,

$$\|\Delta (\mathbf{x}^k - \hat{\mathbf{x}}z_k)\|_2 \leq \|\Delta\|_{\text{op}} \|\mathbf{x}^k - \hat{\mathbf{x}}z_k\|_2.$$

For the third term, we use the right-equivariance of the projection: $\Pi(\mathbf{y}z) = \Pi(\mathbf{y})z$ for $\mathbf{y} \in \mathbb{DH}^n$ and $z \in \text{UDQ}$. Thus,

$$\|\Pi(\mathbf{p}) - \mathbf{r}\|_2 = \left\| \Pi \left(\hat{\mathbf{x}} + \frac{2}{n} \Delta \hat{\mathbf{x}} \right) z_k - \hat{\mathbf{x}}z_k \right\|_2 = \left\| \Pi \left(\hat{\mathbf{x}} + \frac{2}{n} \Delta \hat{\mathbf{x}} \right) - \hat{\mathbf{x}} \right\|_2 \leq 2 \left\| \frac{2}{n} \Delta \hat{\mathbf{x}} \right\|_2,$$

where the inequality follows from Lemma D.3. Combining the bounds gives

$$d(\mathbf{x}^{k+1}, \hat{\mathbf{x}}) \leq \left(\frac{2}{\sqrt{n}} d(\mathbf{x}^k, \hat{\mathbf{x}}) + \frac{4}{n} \|\Delta\|_{\text{op}} \right) d(\mathbf{x}^k, \hat{\mathbf{x}}) + \frac{12}{n} \|\Delta \hat{\mathbf{x}}\|_2. \quad (\text{D.3})$$

Next, we prove by induction that, for all $k = 0, 1, 2, \dots$,

$$d_{st}(\mathbf{x}^k, \hat{\mathbf{x}}) \leq \frac{\sqrt{n}}{25} \quad \text{and} \quad d_{\mathcal{I}}(\mathbf{x}^k, \hat{\mathbf{x}}) \leq \frac{\sqrt{n}}{18}. \quad (\text{D.4})$$

For the base case $k = 0$, the claim follows immediately from Proposition 2.4 with the assumption $\|\Delta\|_{\text{op},st} \leq \frac{n}{350}$, $\|\Delta\|_{\text{op},\mathcal{I}} \leq \frac{n}{300}$. Assume next that (D.4) holds for some $k \geq 0$. It remains to show that $d_{st}(\mathbf{x}^{k+1}, \hat{\mathbf{x}}) \leq \frac{\sqrt{n}}{25}$ and $d_{\mathcal{I}}(\mathbf{x}^k, \hat{\mathbf{x}}) \leq \frac{\sqrt{n}}{18}$. Combining the inductive hypothesis with again the noise assumptions, the standard part for right-hand side of inequality (D.3) and $\|\Delta \hat{\mathbf{x}}\|_2 \leq \sqrt{n} \|\Delta\|_{\text{op}}$ yield

$$\left(\frac{2}{\sqrt{n}} d_{st}(\mathbf{x}^k, \hat{\mathbf{x}}) + \frac{4}{n} \|\Delta\|_{\text{op},st} \right) d_{st}(\mathbf{x}^k, \hat{\mathbf{x}}) + \frac{12}{\sqrt{n}} \|\Delta\|_{\text{op},st} \leq \frac{16}{175} d_{st}(\mathbf{x}^k, \hat{\mathbf{x}}) + \frac{6}{175} \sqrt{n} < \frac{\sqrt{n}}{25},$$

and the dual part for right-hand side of (D.3) is

$$\begin{aligned} & \frac{4}{\sqrt{n}} d_{st}(\mathbf{x}^k, \hat{\mathbf{x}}) d_{\mathcal{I}}(\mathbf{x}^k, \hat{\mathbf{x}}) + \frac{12}{\sqrt{n}} \|\Delta\|_{\text{op}, \mathcal{I}} + \frac{4}{n} (\|\Delta\|_{\text{op}, st} d_{\mathcal{I}}(\mathbf{x}^k, \hat{\mathbf{x}}) + d_{st}(\mathbf{x}^k, \hat{\mathbf{x}}) \|\Delta\|_{\text{op}, \mathcal{I}}) \\ & \leq \frac{4}{\sqrt{n}} \cdot \frac{n}{450} + \frac{12}{\sqrt{n}} \cdot \frac{n}{300} + \frac{4}{n} \left(\frac{n\sqrt{n}}{6300} + \frac{n\sqrt{n}}{7500} \right) < \frac{\sqrt{n}}{18}, \end{aligned}$$

both of which close the induction and proves (D.4) for all $k \geq 0$.

Finally, using (D.3) again together with the fact that $d_{st}(\mathbf{x}^k, \hat{\mathbf{x}}) \leq \frac{\sqrt{n}}{25}$ and $d_{\mathcal{I}}(\mathbf{x}^k, \hat{\mathbf{x}}) \leq \frac{\sqrt{n}}{18}$, we obtain the linear recursion for standard part:

$$d_{st}(\mathbf{x}^k, \hat{\mathbf{x}}) \leq \frac{16}{175} d_{st}(\mathbf{x}^{k-1}, \hat{\mathbf{x}}) + \frac{12}{n} \|\Delta \hat{\mathbf{x}}\|_{2, st}.$$

Unrolling it gives

$$\begin{aligned} d_{st}(\mathbf{x}^k, \hat{\mathbf{x}}) & \leq \left(\frac{16}{175} \right)^k d_{st}(\mathbf{x}^0, \hat{\mathbf{x}}) + \left(1 + \frac{16}{175} + \left(\frac{16}{175} \right)^2 + \dots \right) \frac{12}{n} \|\Delta \hat{\mathbf{x}}\|_{2, st} \\ & \leq \left(\frac{16}{175} \right)^k d_{st}(\mathbf{x}^0, \hat{\mathbf{x}}) + \frac{700}{53n} \|\Delta \hat{\mathbf{x}}\|_{2, st} \\ & < \left(\frac{1}{10} \right)^k d_{st}(\mathbf{x}^0, \hat{\mathbf{x}}) + \frac{700}{53n} \|\Delta \hat{\mathbf{x}}\|_{2, st}. \end{aligned}$$

For the dual part, the recursion relation is

$$d_{\mathcal{I}}(\mathbf{x}^k, \hat{\mathbf{x}}) \leq \frac{28}{225} d_{st}(\mathbf{x}^{k-1}, \hat{\mathbf{x}}) + \frac{16}{175} d_{\mathcal{I}}(\mathbf{x}^{k-1}, \hat{\mathbf{x}}) + \frac{12}{n} \|\Delta \hat{\mathbf{x}}\|_{2, \mathcal{I}}.$$

Unrolling it gives

$$\begin{aligned} d_{\mathcal{I}}(\mathbf{x}^k, \hat{\mathbf{x}}) & \leq \frac{28}{225} \left(\left(\frac{16}{175} \right)^{k-1} d_{st}(\mathbf{x}^0, \hat{\mathbf{x}}) + \frac{700}{53n} \|\Delta \hat{\mathbf{x}}\|_{2, st} \right) + \frac{16}{175} d_{\mathcal{I}}(\mathbf{x}^{k-1}, \hat{\mathbf{x}}) + \frac{12}{n} \|\Delta \hat{\mathbf{x}}\|_{2, \mathcal{I}} \\ & \leq \left(\frac{16}{175} \right)^k d_{\mathcal{I}}(\mathbf{x}^0, \hat{\mathbf{x}}) + \left(1 + \frac{16}{175} + \left(\frac{16}{175} \right)^2 + \dots \right) \left(\frac{12}{n} \|\Delta \hat{\mathbf{x}}\|_{2, \mathcal{I}} + \frac{5}{3n} \|\Delta \hat{\mathbf{x}}\|_{2, st} \right) \\ & \quad + k \left(\frac{16}{175} \right)^{k-1} \frac{28}{225} d_{st}(\mathbf{x}^0, \hat{\mathbf{x}}) \\ & < \left(\frac{1}{10} \right)^k d_{\mathcal{I}}(\mathbf{x}^0, \hat{\mathbf{x}}) + k \left(\frac{1}{10} \right)^{k-1} \frac{1}{8} d_{st}(\mathbf{x}^0, \hat{\mathbf{x}}) + \frac{700}{53n} \|\Delta \hat{\mathbf{x}}\|_{2, \mathcal{I}} + \frac{875}{477n} \|\Delta \hat{\mathbf{x}}\|_{2, st}, \end{aligned}$$

which completes the proof. \square

D.1 Proof of Lemma D.1

We first show that the normalization operator $\mathcal{N}(\cdot)$ is scale-invariant for any nonzero dual quaternion under positive real scaling, i.e.,

$$\mathcal{N}(ax) = \mathcal{N}(x), \quad \forall x \in \mathbb{DH} \setminus \{0\}, \quad a \in \mathbb{R}_{++}. \quad (\text{D.5})$$

If $x_{st} \neq 0$, then by the definition of $\mathcal{N}(\cdot)$ and $|ax_{st}| = a|x_{st}|$, the standard part satisfies

$$\frac{(ax)_{st}}{|(ax)_{st}|} = \frac{ax_{st}}{a|x_{st}|} = \frac{x_{st}}{|x_{st}|},$$

and the image part satisfies

$$\frac{ax_{\mathcal{I}}}{|ax_{st}|} - \frac{ax_{st}}{|ax_{st}|} \text{sc} \left(\frac{(ax_{st})^*(ax_{\mathcal{I}})}{|ax_{st}| |ax_{st}|} \right) = \frac{x_{\mathcal{I}}}{|x_{st}|} - \frac{x_{st}}{|x_{st}|} \text{sc} \left(\frac{x_{st}^* x_{\mathcal{I}}}{|x_{st}| |x_{st}|} \right),$$

which establishes (D.5) in this case.

If $x_{st} = 0$ and $x_{\mathcal{I}} \neq 0$, similarly,

$$\frac{(ax)_{\mathcal{I}}}{|(ax)_{\mathcal{I}}|} = \frac{ax_{\mathcal{I}}}{a|x_{\mathcal{I}}|} = \frac{x_{\mathcal{I}}}{|x_{\mathcal{I}}|},$$

and the feasibility condition for $u_{\mathcal{I}}$ is invariant under positive scaling. Hence, (D.5) holds in this case as well.

Next, we prove that the projection $\Pi(\cdot)$ is scale-invariant under positive real scaling factor for any $\mathbf{y} \in \mathbb{DH}^n$. If $\mathbf{y} = \mathbf{0}$, then $a\mathbf{y} = \mathbf{0}$, and by definition, $\Pi(a\mathbf{y}) = \mathbf{1}^n = \Pi(\mathbf{y})$. Otherwise, let $\tilde{\mathbf{y}} := \Pi(\mathbf{y})$ and $\tilde{\mathbf{y}}_a := \Pi(a\mathbf{y})$. For each index i , if $y_i \neq 0$, then $(a\mathbf{y})_i \neq 0$, and by (D.5),

$$[\tilde{\mathbf{y}}_a]_i = \mathcal{N}((a\mathbf{y})_i) = \mathcal{N}(ay_i) = \mathcal{N}(y_i) = \tilde{y}_i.$$

If $y_i = 0$, the definition uses $\mathcal{N}(\mathbf{e}^*\mathbf{y})$ for any \mathbf{e} with $\mathbf{e}^*\mathbf{y} \neq 0$. Since $a > 0$, the same \mathbf{e} satisfies $\mathbf{e}^*(a\mathbf{y}) = a(\mathbf{e}^*\mathbf{y}) \neq 0$, and again by (D.5),

$$[\tilde{\mathbf{y}}_a]_i = \mathcal{N}(\mathbf{e}^*(a\mathbf{y})) = \mathcal{N}(a(\mathbf{e}^*\mathbf{y})) = \mathcal{N}(\mathbf{e}^*\mathbf{y}) = \tilde{y}_i.$$

Thus, $\Pi(a\mathbf{y}) = \Pi(\mathbf{y})$ for all $a \in \mathbb{R}_{++}$ and $\mathbf{y} \in \mathbb{DH}^n$.

D.2 Proof of Lemma D.2

Notation used in this proof: For given $\mathbf{u} = (u_1, u_2, \dots, u_n), \mathbf{v} = (v_1, v_2, \dots, v_n) \in \mathbb{DH}^n$, with $u_i = u_{i,st} + u_{i,\mathcal{I}}\epsilon, v_i = v_{i,st} + v_{i,\mathcal{I}}\epsilon$. Denote $\langle \mathbf{u}, \mathbf{v} \rangle$ as $(\mathbf{u}^*\mathbf{v} + \mathbf{v}^*\mathbf{u})/2$. Thus we have

$$\langle \mathbf{u}, \mathbf{v} \rangle = \sum_{i=1}^n \text{sc}(u_{i,st} v_{i,st}^*) + \sum_{i=1}^n (\text{sc}(u_{i,st} v_{i,\mathcal{I}}^*) + \text{sc}(v_{i,st} u_{i,\mathcal{I}}^*))\epsilon.$$

Let $\mathbf{z} := \Pi(\mathbf{x} + \Pi(\mathbf{x}) + \mathbf{y})$. From the definition of $\Pi(\cdot)$, taking $\Pi(\mathbf{x})$ as a feasible point, we have

$$\|\mathbf{x} + \Pi(\mathbf{x}) + \mathbf{y} - \mathbf{z}\|_2^2 \leq \|\mathbf{x} + \Pi(\mathbf{x}) + \mathbf{y} - \Pi(\mathbf{x})\|_2^2. \quad (\text{D.6})$$

Using $\|\mathbf{u} - \mathbf{v}\|_2^2 = \|\mathbf{u}\|_2^2 + \|\mathbf{v}\|_2^2 - 2\langle \mathbf{u}, \mathbf{v} \rangle$ for any \mathbf{u}, \mathbf{v} and $\|\mathbf{z}\|_2^2 = \|\Pi(\mathbf{x})\|_2^2 = n$ (since $\mathbf{z}, \Pi(\mathbf{x}) \in \text{UDQ}^n$), inequality (D.6) simplifies to

$$\langle \mathbf{y}, \mathbf{z} - \Pi(\mathbf{x}) \rangle \geq \langle \mathbf{x} + \Pi(\mathbf{x}), \Pi(\mathbf{x}) - \mathbf{z} \rangle. \quad (\text{D.7})$$

On the other hand, since $\Pi(\mathbf{x})$ is the projection of \mathbf{x} onto UDQ^n and $\mathbf{z} \in \text{UDQ}^n$,

$$\|\mathbf{x} - \Pi(\mathbf{x})\|_2^2 \leq \|\mathbf{x} - \mathbf{z}\|_2^2,$$

which implies

$$\langle \mathbf{x}, \Pi(\mathbf{x}) - \mathbf{z} \rangle \geq 0. \quad (\text{D.8})$$

Combining (D.7) and (D.8), we obtain

$$\langle \mathbf{y}, \mathbf{z} - \Pi(\mathbf{x}) \rangle \geq \langle \mathbf{x} + \Pi(\mathbf{x}), \Pi(\mathbf{x}) - \mathbf{z} \rangle = \langle \mathbf{x}, \Pi(\mathbf{x}) - \mathbf{z} \rangle + \langle \Pi(\mathbf{x}), \Pi(\mathbf{x}) - \mathbf{z} \rangle \geq \langle \Pi(\mathbf{x}), \Pi(\mathbf{x}) - \mathbf{z} \rangle.$$

Moreover,

$$\langle \Pi(\mathbf{x}), \Pi(\mathbf{x}) - \mathbf{z} \rangle = \langle \Pi(\mathbf{x}), \Pi(\mathbf{x}) \rangle - \langle \Pi(\mathbf{x}), \mathbf{z} \rangle = n - \langle \Pi(\mathbf{x}), \mathbf{z} \rangle = \frac{1}{2} \|\Pi(\mathbf{x}) - \mathbf{z}\|_2^2.$$

Hence

$$\langle \mathbf{y}, \mathbf{z} - \Pi(\mathbf{x}) \rangle \geq \frac{1}{2} \|\Pi(\mathbf{x}) - \mathbf{z}\|_2^2 \geq 0. \quad (\text{D.9})$$

By the Cauchy–Schwarz inequality (e.g., Proposition 4.7 in [Ling et al. \(2022\)](#)),

$$\langle \mathbf{y}, \mathbf{z} - \Pi(\mathbf{x}) \rangle \leq \|\mathbf{y}\|_2 \|\mathbf{z} - \Pi(\mathbf{x})\|_2.$$

Together with (D.9), this yields

$$\frac{1}{2} \|\mathbf{z} - \Pi(\mathbf{x})\|_2^2 \leq \|\mathbf{y}\|_2 \|\mathbf{z} - \Pi(\mathbf{x})\|_2.$$

If $\|\mathbf{z} - \Pi(\mathbf{x})\|_2 = 0$, the claim is trivial. Otherwise, factoring out the term $\|\mathbf{z} - \Pi(\mathbf{x})\|_2$, we obtain

$$\|\mathbf{z} - \Pi(\mathbf{x})\|_2 \cdot \left(\frac{1}{2} \|\mathbf{z} - \Pi(\mathbf{x})\|_2 - \|\mathbf{y}\|_2 \right) \leq 0.$$

Since norms are non-negative, the second factor must be non-positive, i.e.,

$$\|\mathbf{z} - \Pi(\mathbf{x})\|_2 \leq 2\|\mathbf{y}\|_2,$$

which proves the lemma.

D.3 Proof of Lemma D.3

By the triangle inequality,

$$\|\Pi(\mathbf{p} + \mathbf{q}) - \mathbf{r}\|_2 \leq \|\Pi(\mathbf{p} + \mathbf{q}) - \Pi(\mathbf{p})\|_2 + \|\Pi(\mathbf{p}) - \mathbf{r}\|_2.$$

Applying Lemma D.2 with $\mathbf{x} = \mathbf{p}$ and $\mathbf{y} = \mathbf{q} - \Pi(\mathbf{p})$ yields

$$\|\Pi(\mathbf{p} + \mathbf{q}) - \Pi(\mathbf{p})\|_2 = \|\Pi(\mathbf{p} + \Pi(\mathbf{p}) + (\mathbf{q} - \Pi(\mathbf{p}))) - \Pi(\mathbf{p})\|_2 \leq 2\|\mathbf{q} - \Pi(\mathbf{p})\|_2.$$

Finally, using the triangle inequality again,

$$\|\mathbf{q} - \Pi(\mathbf{p})\|_2 \leq \|\mathbf{q} - \mathbf{r}\|_2 + \|\Pi(\mathbf{p}) - \mathbf{r}\|_2.$$

Combining the above three displays gives (D.1).

D.4 Proof of Lemma D.4

Let $s_k := \hat{\mathbf{x}}^* \mathbf{x}^k \in \mathbb{DH}$ and define $p_k := z_k^* s_k$. Since $|z_k| = 1$, we have

$$|\hat{\mathbf{x}}^* \mathbf{x}^k - n z_k| = |z_k^* (\hat{\mathbf{x}}^* \mathbf{x}^k - n z_k)| = |p_k - n|.$$

On the other hand,

$$d(\mathbf{x}^k, \hat{\mathbf{x}})^2 = \|\mathbf{x}^k - \hat{\mathbf{x}} z_k\|_2^2 = 2n - (p_k + p_k^*),$$

where we used $\|\mathbf{x}^k\|_2^2 = \|\hat{\mathbf{x}} z_k\|_2^2 = n$ and the definition of the inner product.

Therefore it suffices to show that p_k is Hermitian and satisfies $0 \preceq p_k \preceq n + 0\epsilon$ (in the total order on dual numbers). In that case,

$$\frac{1}{2} d(\mathbf{x}^k, \hat{\mathbf{x}})^2 = n - \frac{p_k + p_k^*}{2} = n - p_k = |n - p_k| = |p_k - n|,$$

which yields the desired identity.

It remains to justify that p_k is a dual number (i.e., $p_k = p_k^*$) and $0 \preceq p_k \preceq n + 0\epsilon$. Write $s_k = a_k + b_k\epsilon$ and $z_k^* = c_k + d_k\epsilon$ with $a_k, b_k, c_k, d_k \in \mathbb{H}$. The constraint $z_k \in \text{UDQ}$ implies $c_k^*c_k = 1$ and $d_kc_k^* + c_kd_k^* = 0$. Moreover, z_k is chosen to minimize $\|\mathbf{x}^k - \hat{\mathbf{x}}z\|_2^2$, which is equivalent to maximizing the dual number $p + p^*$ over $z \in \text{UDQ}$.

Case 1: $a_k \neq 0$. Maximizing the standard (rotation) part yields

$$c_k = \frac{a_k^*}{|a_k|}, \quad \text{so that} \quad \text{st}(c_k a_k) = |a_k| \in \mathbb{R}_{\geq 0}.$$

With this choice, the UDQ constraint $d_k c_k^* + c_k d_k^* = 0$ is equivalent to

$$d_k a_k + a_k^* d_k^* = 0,$$

i.e., $d_k a_k$ can be any pure quaternion. Moreover,

$$p_k = (c_k + d_k\epsilon)(a_k + b_k\epsilon) = |a_k| + \left(\frac{a_k^* b_k}{|a_k|} + d_k a_k \right) \epsilon.$$

We choose d_k so that the ϵ -coefficient is real, namely,

$$d_k a_k = -\text{im}\left(\frac{a_k^* b_k}{|a_k|}\right),$$

which is feasible since the right-hand side is a pure quaternion (with $\text{im}(\cdot)$ denoting the imaginary vector part). With this choice, the ϵ -coefficient reduces to $\text{sc}\left(\frac{a_k^* b_k}{|a_k|}\right) \in \mathbb{R}$, hence $p_k \in \mathbb{D} = \mathbb{R} + \epsilon\mathbb{R}$ and in particular $p_k = p_k^*$. Furthermore, since $|z_k| = 1$ and by Cauchy–Schwarz,

$$|p_k| = |z_k^* s_k| \leq |s_k| = |\hat{\mathbf{x}}^* \mathbf{x}^k| \leq \|\hat{\mathbf{x}}\|_2 \|\mathbf{x}^k\|_2 = n,$$

and $\text{st}(p_k) \geq 0$ by construction. Therefore $0 \preceq p_k \preceq n + 0\epsilon$ under the standard order on dual numbers.

Case 2: $a_k = 0$. Then $s_k = b_k\epsilon$ has zero standard part, so the objective $z^* s_k + (z^* s_k)^*$ has zero standard part for every $z \in \text{UDQ}$. We may thus adopt an arbitrary tie-breaking rule to select an optimizer z_k . In this case $p_k = z_k^* s_k$ is purely infinitesimal (i.e., $\text{st}(p_k) = 0$), and the identity above still yields

$$\frac{1}{2} d(\mathbf{x}^k, \hat{\mathbf{x}})^2 = n = |p_k - n|.$$

The proof is complete.

D.5 Proof of Corollary 3.4

Denote the sequence generated by Algorithm 1 as $\{\mathbf{w}^k\}_{k \geq 0}$. Write \mathbf{w}^0 as $\mathbf{w}^0 = \sum_{i=1}^n \mathbf{v}_i \alpha_j$, where $\mathbf{v}_1, \dots, \mathbf{v}_n$ are orthonormal eigenvectors of C corresponding to $\lambda_1, \dots, \lambda_n$ respectively. Suppose $\lambda_{1,\text{st}} > 0$ and $|\alpha_{1,\text{st}}| \neq 0$. Since Algorithm 1 is a (normalized) power iteration, we can write

$$\mathbf{w}^k = \sum_{j=1}^n \mathbf{v}_j t_j^k, \quad t_j^k := \lambda_j^k \alpha_j \left(\sqrt{\sum_{\ell=1}^n |\lambda_{\ell}^k \alpha_{\ell}|^2} \right)^{-1}.$$

As $k \rightarrow \infty$, using $|\lambda_{1,st}| > |\lambda_{2,st}|$ and standard dual-number expansion,

$$\begin{aligned}
& \sqrt{\sum_{j=1}^n |\lambda_j^k \alpha_j|^2 - |\lambda_1|^k |\alpha_1|} \\
& \left(\sqrt{\sum_{j=1}^n |\lambda_j^k \alpha_j|^2 - |\lambda_1|^k |\alpha_1|} \right) \left(\sqrt{\sum_{j=1}^n |\lambda_j^k \alpha_j|^2 + |\lambda_1|^k |\alpha_1|} \right) \left(\sqrt{\sum_{j=1}^n |\lambda_j^k \alpha_j|^2 + |\lambda_1|^k |\alpha_1|} \right)^{-1} \\
& = \sum_{j=2}^n |\lambda_j^k \alpha_j|^2 \left(\sqrt{\sum_{j=1}^n |\lambda_j^k \alpha_j|^2 + |\lambda_1|^k |\alpha_1|} \right)^{-1} \\
& = \sum_{j=2}^n |\lambda_{j,st}|^{2k} (1 + 2k\lambda_{j,st}^{-1} \lambda_{j,\mathcal{I}} \epsilon) |\alpha_j|^2 A^{-1} \\
& = O_D \left(\left(\frac{\lambda_{2,st}^2}{\lambda_{1,st}} \right)^k \right),
\end{aligned}$$

where

$$A := \left(\sum_{j=1}^n |\lambda_{j,st}|^{2k} (1 + 2k\lambda_{j,st}^{-1} \lambda_{j,\mathcal{I}} \epsilon) |\alpha_j|^2 \right)^{1/2} + |\lambda_{1,st}|^k (1 + k\lambda_{1,st}^{-1} \lambda_{1,\mathcal{I}} \epsilon) |\alpha_1|.$$

This implies

$$t_j^k = \lambda_j^k \alpha_j \left[|\lambda_1|^k |\alpha_1| + O_D \left((|\lambda_{2,st}|^2 / |\lambda_{1,st}|)^k \right) \right]^{-1}.$$

For $j = 1$, since $\lambda_1 > 0$ we have $\lambda_1^k / |\lambda_1|^k = 1$, then

$$\begin{aligned}
t_1^k - \lambda_1^k \alpha_1 \left(|\lambda_1|^k |\alpha_1| \right)^{-1} &= \lambda_1^k \alpha_1 \left[|\lambda_1|^k |\alpha_1| + O_D \left((|\lambda_{2,st}|^2 / |\lambda_{1,st}|)^k \right) \right]^{-1} - \lambda_1^k \alpha_1 \left(|\lambda_1|^k |\alpha_1| \right)^{-1} \\
&= -\lambda_1^k \alpha_1 \left(|\lambda_1|^k |\alpha_1| \right)^{-1} \cdot O_D \left((|\lambda_{2,st}|^2 / |\lambda_{1,st}|)^k \right) \left[|\lambda_1|^k |\alpha_1| + O_D \left((|\lambda_{2,st}|^2 / |\lambda_{1,st}|)^k \right) \right]^{-1} \\
&= -\alpha_1 |\alpha_1|^{-1} \cdot O_D \left((|\lambda_{2,st}|^2 / |\lambda_{1,st}|)^k \right) \left[|\lambda_1|^k |\alpha_1| + O_D \left((|\lambda_{2,st}|^2 / |\lambda_{1,st}|)^k \right) \right]^{-1}.
\end{aligned}$$

Thus, we have

$$\begin{aligned}
\mathbf{w}^k &= \mathbf{v}_1 \alpha_1 |\alpha_1|^{-1} \left\{ 1 - O_D \left((|\lambda_{2,st}|^2 / |\lambda_{1,st}|)^k \right) \left[|\lambda_1|^k |\alpha_1| + O_D \left((|\lambda_{2,st}|^2 / |\lambda_{1,st}|)^k \right) \right]^{-1} \right\} \\
&\quad + \sum_{j=2}^n \mathbf{v}_j \lambda_j^k \alpha_j \left(|\lambda_1|^k |\alpha_1| + O_D \left((|\lambda_{2,st}|^2 / |\lambda_{1,st}|)^k \right) \right)^{-1}.
\end{aligned}$$

Using the distance definition and the feasible choice $z = \alpha_1 |\alpha_1|^{-1} \in \text{UDQ}$,

$$\begin{aligned}
\text{d}(\mathbf{w}^k, \mathbf{v}_1) &= \min_{z \in \text{UDQ}} \|\mathbf{w}^k - \mathbf{v}_1 z\|_2 \leq \left\| \mathbf{w}^k - \mathbf{v}_1 \alpha_1 |\alpha_1|^{-1} \right\|_2 \\
&\leq \|\mathbf{v}_1\|_2 O_D \left((|\lambda_{2,st}|^2 / |\lambda_{1,st}|)^k \right) \left[|\lambda_1|^k |\alpha_1| + O_D \left((|\lambda_{2,st}|^2 / |\lambda_{1,st}|)^k \right) \right]^{-1} \\
&\quad + \sum_{j=2}^n \|\mathbf{v}_j\|_2 |\lambda_j|^k |\alpha_j| \left[|\lambda_1|^k |\alpha_1| + O_D \left((|\lambda_{2,st}|^2 / |\lambda_{1,st}|)^k \right) \right]^{-1} \\
&= \left[\sum_{j=2}^n |\lambda_j|^k |\alpha_j| + O_D \left((|\lambda_{2,st}|^2 / |\lambda_{1,st}|)^k \right) \right] \left[|\lambda_1|^k |\alpha_1| + O_D \left((|\lambda_{2,st}|^2 / |\lambda_{1,st}|)^k \right) \right]^{-1}.
\end{aligned} \tag{D.10}$$

We use $\sqrt{n}\mathbf{w}^k$ as an initializer for Algorithm 2. As in the proof of Theorem 3.2, it suffices to enforce

$$d_{st}(\mathbf{w}^k, \mathbf{v}_1) \leq \frac{1}{35}, \quad d_{\mathcal{I}}(\mathbf{w}^k, \mathbf{v}_1) \leq \frac{1}{25}, \quad (\text{D.11})$$

to guarantees that $\sqrt{n}\mathbf{w}^k$ enters the basin of attraction with

$$d_{st}(\sqrt{n}\mathbf{w}^k, \hat{\mathbf{x}}) \leq d_{st}(\sqrt{n}\mathbf{w}^k, \sqrt{n}\mathbf{v}_1) + d_{st}(\sqrt{n}\mathbf{v}_1, \hat{\mathbf{x}}) \leq \frac{\sqrt{n}}{25}$$

and

$$d_{\mathcal{I}}(\sqrt{n}\mathbf{w}^k, \hat{\mathbf{x}}) \leq d_{\mathcal{I}}(\sqrt{n}\mathbf{w}^k, \sqrt{n}\mathbf{v}_1) + d_{\mathcal{I}}(\sqrt{n}\mathbf{v}_1, \hat{\mathbf{x}}) \leq \frac{\sqrt{n}}{18}.$$

By the dual quaternion calculation rules, for all sufficiently large k there exist real constants $M_{st}, M_{\mathcal{I}}, N_1, N_2$, such that

$$d_{st}(\mathbf{w}^k, \mathbf{v}_1) = \frac{|\lambda_{2,st}|^k |\alpha_{2,st}| + M_{st} |\lambda_{2,st}|^k}{|\lambda_{1,st}|^k |\alpha_{1,st}| + M_{st} |\lambda_{2,st}|^k}, \quad (\text{D.12})$$

and

$$d_{\mathcal{I}}(\mathbf{w}^k, \mathbf{v}_1) = \frac{N_2 |\lambda_{2,st}|^k + M_{\mathcal{I}} |\lambda_{2,st}|^k}{N_1 |\lambda_{1,st}|^k + M_{\mathcal{I}} |\lambda_{2,st}|^k}. \quad (\text{D.13})$$

Specifically,

$$\begin{aligned} M_{st} &= M_{st}(\alpha_{1,st}, \lambda_{1,st}, \lambda_{1,\mathcal{I}}), & M_{\mathcal{I}} &= M_{\mathcal{I}}(\alpha_{1,st}, \alpha_{1,\mathcal{I}}, \lambda_{1,st}, \lambda_{1,\mathcal{I}}), \\ N_1 &= N_1(\lambda_{1,st}, \lambda_{1,\mathcal{I}}, \alpha_{1,st}), & N_2 &= N_2(\lambda_{2,st}, \lambda_{2,\mathcal{I}}, \alpha_{2,st}). \end{aligned}$$

Let $r := |\lambda_{1,st}/\lambda_{2,st}| > 1$. Solving (D.12)–(D.13) under (D.11) yields

$$K_{\text{init}} \geq \max \left\{ \log_r \left(\frac{35|\alpha_{2,st}| + 34M_{st}}{|\alpha_{1,st}|} \right), \log_r \left(\frac{25N_2 + 24M_{\mathcal{I}}}{N_1} \right) \right\}.$$

With K_{init} iterations, the initial point \mathbf{x}^0 satisfies the basin of attraction conditions:

$$d_{st}(\mathbf{x}^0, \hat{\mathbf{x}}) \leq \frac{\sqrt{n}}{25}, \quad d_{\mathcal{I}}(\mathbf{x}^0, \hat{\mathbf{x}}) \leq \frac{\sqrt{n}}{18}.$$

Substituting these bounds into the estimation error recursive formulas derived in Theorem 3.2 (specifically Eq. (3.1) and Eq. (3.2)) directly yields the claimed error bounds for \mathbf{x}^k . This completes the proof.